Modeling Methylmercury in Maine's Tribal Meres

by

Nick Hoffman

Submitted to the Department of Earth, Atmospheric, and Planetary Sciences in Partial Fulfillment of the Requirements for the Degree of Bachelor of Science in Earth, Atmospheric, and Planetary Sciences at the Massachusetts Institute of Technology

May 11, 2018 [June 2018]

Author Signature redacted
Department of Earth, Atmospheric and Planetary Sciences
May 11, 2018

Certified by Signature redacted
Noelle Selin
Thesis Supervisor

Accepted by Signature redacted
Richard P. Binzel
Chair, Committee on Undergraduate Program

0. ABSTRACT

Methylmercury (MeHg) concentrations in the fish of twenty Maine lakes were projected for the year 2035 under three different policy scenarios. A mechanistic model of Hg fate and transport was calibrated for Maine's environment using four parameters: volumetric outflow rate, settling velocity, burial velocity, and Hg(II) biotic solids partitioning coefficient. The model was evaluated through comparison with measured results from the year 1993. The model results showed that the strictest global Hg regulations will lead to the greatest decreases in MeHg concentration. No piscivore will be safe for frequent consumption, even under the strictest regulations in the cleanest lakes. The Wabanaki traditional-subsistence diet will continue to entail unsafe MeHg exposures.

I. INTRODUCTION

Global atmospheric mercury (Hg) concentrations have been enriched by a factor of 2.6 since the Industrial Revolution as a result of coal-burning, artisanal and small-scale gold mining, smelting, waste incineration, and biomass burning, among other human causes (Amos et al. 2013). Hg travels regionally and globally via the atmosphere in its gaseous elemental form (Hg(0)) and deposits to ecosystems as Hg(II). The major long-term sink of mercury is marine sediment burial, but this sink acts slowly because of the slow rate of ocean circulation (Selin, 2009). Therefore, circulating mercury has accumulated to the point that one tenth of current emissions is natural, 30% is due to current anthropogenic activity, and 60% are due to historical anthropogenic emissions (Amos et al. 2013).

Hg(II) in the sediment and water column of aquatic ecosystems can be converted into methylmercury (MeHg) by iron- and sulfate-reducing bacteria (Jensen & Jernelöv, 1969; Knightes et al. 2009). MeHg is both neurotoxic and cardiotoxic, and it bioaccumulates

in fish, such that fish higher in the food web have higher MeHg levels (Eagles-smith et al. 2018). Human consumption of fish is a major exposure pathway to MeHg.

Rates of fish consumption, as well as kinds of fish consumed, vary widely and systematically among the US population. Whereas fish forms only a marginal component of diet for many Americans, some groups such as Native American tribes, will eat fish as frequently as daily (EPA, 2009; O'Neill, 2004). Further, for many Native American groups, fishing is an important component of cultural and religious practice (EPA, 2009). Therefore, increased MeHg concentration in fish poses special risks for tribal populations and is an issue relevant to environmental justice. A better understanding of the sensitivity of mercury concentration in fish to local, national, and global variables will facilitate safe navigation between current and desired levels of fish consumption among Native populations, guiding policy that will promote cultural self-determination for Native groups.

The objective of this study was to better understand the potential future (2035) concentration of methylmercury (MeHg) in Maine freshwater fish under three different policy scenarios, through the calibration of a Hg fate and transport model. The lakes studied are those used by the Wabanaki tribes as a source of food, for which data have been collected for the year 1993 in the USGS study, "Fish Tissue in Maine Lakes Contamination Report" (Maine DEP, 1995). A list and map of these lakes can be found in the appendix. The model used was based on the Spreadsheet-based Ecological Risk Assessment for the Fate of Mercury (SERAFM), a mechanistic model of mercury accumulation in lake fish developed by the Environmental Protection Agency (EPA) (Knightes et al. 2009). The particular implementation of SERAFM used was developed by Hendricks (2018) in the programming language R, modified to enable prediction of lake responses to changes in loadings. The

model was calibrated to the environmental conditions specific to Maine's lakes. The three policy scenarios studied – current policy (CP), new policy (NP), and maximum feasible reduction (MFR) – were taken from Pacyna et al. (2016) to represent the effect in 2035 of increasingly strict global regulations on mercury emissions.

II. MERCURY BIOGEOCHEMICAL CYCLE - REVIEW OF LITERATURE

The element mercury (Hg) is mobilized naturally via tectonic activity and volcanism from deep reservoirs, and it circulates between the atmosphere, the land, and the water (Gustin et al. 2000). However, the natural flux of Hg has been augmented by human interference in the Hg cycle. Through both intentional uses, like artisanal small-scale gold mining (ASGM), and unintentional releases, as in coal burning, human activities are estimated to have enriched the atmosphere by a factor of 7.5 from 2000 BC levels (Amos et al. 2013). Given Hg's centuries-long lifetime against land sequestration and marine deep sediment burial, anthropogenic emissions of Hg continue to cycle for centuries to millennia and are referred to as legacy emissions (Fitzgerald et al. 2007; Nriagu, 1993).

The increase in the Hg flux caused by human activities is a problem because of Hg's negative impacts on the health of humans and wildlife. In the form of methylmercury (MeHg), this chemical is particularly neurotoxic, with particularly adverse effects for the offspring of exposed pregnant women (Grandjean et al, 2010; UNEP, 2002; Selin, 2009). MeHg also has neurotoxic, immunotoxic, and genotoxic effects on wildlife, from other mammals, to birds, to fish (Wolfe, Schwarzbach and Sulaiman, 1998). MeHg bioaccumulates in the muscles of the animals that consume it, and it biomagnifies, increasing in concentration with the trophic status of the organism that consumes it (Boening, 2000). For many human populations, fish consumption is the main source of

exposure to MeHg (Sunderland et al. 2018). This toxic chemical poses a particularly difficult problem for those communities that consume large amounts of fish, such as subsistence fishers (AMAP, 2015) and many Native American bands (EPA, 2009).

In order to navigate the gap between safe and desired consumption levels for populations with significant exposure to MeHg, it is necessary to model changes in the concentration of MeHg in fish over time (Gagnon et al. 2017). In particular, for Maine's Wabanaki Confederacy, whose traditional-subsistence diet includes many fish such as sturgeon, mackerel, trout, and whitefish, modeling must take the particular environmental conditions of Maine's lake ecosystems into account (EPA, 2009). Although some lake Hg pollution can be attributed to direct inputs from local sources, this review focuses on pollution in remote lakes, where the main source of contamination is deposition from the global Hg pool. Some parts of Maine – such as the Penobscot River and its catchment – have been contaminated with Hg by tanning and pulping factories (Yeager et al. 2018; Santschi et al. 2017). However, according to the 2011 National Emissions Inventory (NEI), Hg emissions from tribal lands in Maine's remote eastern regions are insignificant (NEI, 2011). Looking at changes in US and global anthropogenic emissions is relevant to American policymakers, who can control American emissions relatively easily, and who can help regulate background Hg emissions coming from global well-mixed elemental Hg (Hg(0)) through their participation in the multilateral Minamata Convention on Mercury, which has been ratified by 92 parties and entered into force in the summer of 2017 (UNEP, 2013b). This review presents the current state of knowledge on the emissions, transport, and fate of Hg (see Fig. 2.1.1), with a particular focus on the dynamics of Hg cycling in lake ecosystems.

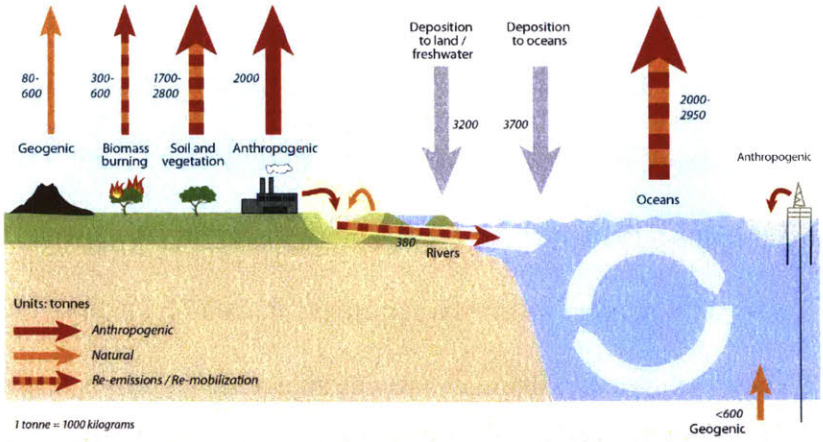

Figure 2.1.1: The Mercury Cycle. From UNEP (2013a). The anthropogenic flux to the atmosphere, broadly conceived (current anthropogenic and legacy emissions), may be as much as 21x the natural flux, taking the middle value from each range in the figure above. Amos et al. (2013) writes that it is 9x.

2.1. Atmospheric cycle

2.1.1. Emissions

Hg emissions are divided into a natural, anthropogenic, and legacy component. The natural component accounts for 10%, the anthropogenic component for 30%, and the legacy component for 60% of the total magnitude of annual emissions (Amos et al. 2013).

Natural sources of atmospheric Hg include evasion from the global mercury belt (see Fig. 2.1.2), volcanism, natural evasion from water, and natural forest fires. However, all of these sources of Hg, except for the geogenic flux, have been influenced by human activity. Anthropogenic emissions have cycled through terrestrial and aquatic ecosystems; only the fluxes from the mercury belt and volcanism are completely primary (Fitzgerald & Lamborg, 2013).

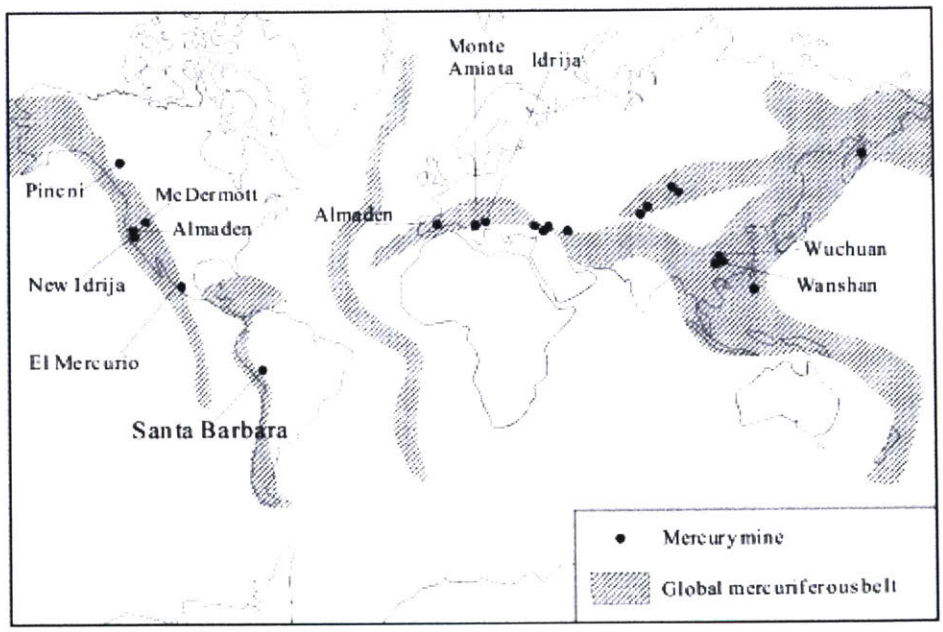

Figure 2.1.2: The Global Mercury Belt. From Wang et al. (2005). Subduction zones are surrounded by rock enriched in volatile mercury ores. In total, they contribute a relatively small portion of yearly Hg emissions.

The global mercury belt begins at the southern tip of South America, wraps around the Pacific rim, follows the Himalayas through India, and ends in Spain (Gustin et al. 2000). This belt, reflecting major subduction zones, comprises minerals, such as sphalerite and chalcopyrite, enriched in mercury (Fitzgerald & Lamborg, 2013). Because of the extreme volatility of Hg(0), this belt emits significant amounts of mercury yearly. Scaling up Gustin et al. (2000)'s study of the Western US, Fitzgerald and Lamborg (2013) suggest a global flux from the mercury belt on the order of 1000 tons per year, on the high side of estimates. Selin (2009) documents estimates ranging between 75 and 700 tons per year.

Ferrara et al. (2000) calculated the flux of Hg from volcanoes using the ratio of sulfur (S) to Hg in the plume, and they found the yearly flux from Mount Etna to be between 0.6 and 5 tons. Fitzgerald and Lamborg (2013) compiled a range of estimates of the global flux from volcanoes, none of which were greater than 100 tons per year.

Anthropogenic emissions of mercury come from mining, fossil fuel combustion, industrial processes, medical waste incineration, and biomass burning (Fitzgerald & Lamborg, 2013). Cooke et al. (2009) documents mining of cinnabar (HgS) at the Huancavelica mine in the Peruvian Andes as early as 1400 BC, with peak levels occurring at the height of the Chavín and Inca states, in 500 BC and 1450 AD respectively. Pacyna and Pacyna (2002) estimate that for the year 1995, roughly three quarters of the total anthropogenic flux of Hg was due to stationary combustion of Hg-containing fuels. In total, they estimate that the 1995 anthropogenic flux was approximately 2000 tons. For the year 2010, anthropogenic emissions totaled 1960 tons, 37% of which was from ASGM, 32% from mining, smelting, and metal production, and 24% from coal burning (UNEP, 2013b). One third of 2010's global total came from China (Streets et al. 2011; UNEP, 2013b Streets et al. 2017). While Hg emissions in the US have been decreasing since the 1990s due to domestic regulation, they have been increasing in East Asia with increasing coal burning (Selin, 2009; Pacyna et al. 2016). Pacyna et al. (2016) suggests that if the Minamata Convention on Mercury is fully implemented, Hg deposition in 2035 will decrease globally by 20-30%, except for in South Asia (e.g., India), where deposition will increase by 10-15%. This moderate Asian increase is an improvement on the 50% increase in South and East Asia projected to occur if governments fail to implement the Minamata Convention (Pacyna et al. 2016).

Hg tends to deposit on the surface of terrestrial and aquatic ecosystems, where it will be partially re-emitted alongside a natural component. This re-emitted component is referred to as legacy or historical emissions and should be considered human-caused (Fitzgerald & Lamborg, 2013). In aquatic environments, Hg(II) is reduced to Hg(0) before

revolatilizing (O'Driscoll et al. 2017). More recently deposited Hg is more available for re-emission because it does not have time to bind with organic matter in terrestrial ecosystems. This preferential recycling of newly deposited Hg is referred to as prompt recycling (Selin, 2009; Hintelmann et al. 2002).

2.1.2. Transport and chemical transformation

Mercury is emitted into the atmosphere in three forms: elemental (Hg(0)), divalent (Hg(II)), and particulate-bound (Hg(P)). Natural sources of Hg are exclusively elemental, but anthropogenic sources comprise all three forms (Selin, 2009).

Greater than 90% of total atmospheric mercury is in its elemental form, which mixes well globally due to its long lifetime (roughly 0.5-1 year) (Selin, 2009; Horowitz et al. 2017). Average background concentrations of Hg(0) are about 1.5 ng/m^3 in the northern hemisphere, and range between 0.9 and 1.0 ng/m^3 in the southern hemisphere (Sprovieri et al. 2016).

Hg(II) makes up about 3% of total gaseous mercury and deposits regionally, downwind of its emission sites, due to its short lifetime against rainout (on the order of several days) (Lin and Pehkonen, 1999; Lindqvist and Rodhe, 1985). Poissant et al. (2008) measured mean concentrations of Hg(II) at the St. Anicet site in Québec as 2.2 pg/m^3, with a standard deviation of 3.7 in 2004. Lindberg and Stratton (1998) measured mean concentration of Hg(II) in Tennessee at 92 pg/m^3, and in Indiana at 104 pg/m^3 with standard deviations of 60 pg/m^3 and 57 pg/m^3, respectively. These regional differences demonstrate how the concentration of Hg(II) in remote locations can be reduced compared to its concentration near emission sources. Hg(II) concentration increases with elevation, and it peaks during midday (Shah et al. 2016; Shah & Jaeglé, 2017; Fu et al. 2016). Hg(P) is

variable in its concentration; it can be as much as 40% of total mercury near emission sites, but it tends to be on the order of 1% in general (Lin and Pehkonen, 1999; Xiao et al. 1991). At St. Anicet, Hg(P) was measured at 3.4 pg/m^3, with a standard deviation of 5.2 (Poissant et al. 2008). Hg(P) also deposits regionally.

Although most atmospheric Hg exists as Hg(0), it can be oxidized to Hg(II) (Selin, 2009). Hg(II) converts to Hg(P) with decreasing temperature and increasing particulate matter (PM) loading (Amos et al. 2012). Although earlier studies suggested that the oxidizing agent was ozone or the hydroxyl radical (Sommar et al. 2001), newer work suggests bromine is the primary oxidant of Hg (Holmes et al. 2010; Horowitz et al. 2017). Holmes et al. (2010) found that a global chemical model incorporating oxidation by Br better simulates the depletion and subsequent rebound of gaseous Hg(0) concentrations in the polar regions in the spring and summer. Horowitz et al. (2017) further suggest that Hg(0)'s lifetime has been overestimated, offering an estimate of roughly half a year. In addition to the oxidation of Hg(0) to Hg(II), some Hg(II) gets reduced in the atmosphere back to Hg(0) (Selin et al. 2007; Horowitz et al. 2017).

2.1.3. Deposition

Deposition of Hg in a particular region depends on the magnitude and speciation of domestic and foreign emissions, and on the oxidative capacity of the atmosphere that transforms Hg(0) to divalent species. Due to different physico-chemical properties, Hg(0) mainly deposits through dry deposition, while Hg(II) and Hg(P) tend to enter aquatic ecosystems through wet deposition. Selin and Jacob (2008) estimate that wet deposition contributes 30% to the total magnitude of Hg deposition in the US, with the rest being dry.

In the mid-latitudes, dry deposition occurs 95-98% of the time, while wet deposition occurs the other 2-5% of the time (Lindberg et al. 2007).

Wet deposition occurs when rainfall scavenges Hg(II) and Hg(P), and a small amount (0.5-2.5 %) of MeHg (Lindberg et al. 2007). Hg(P), but not Hg(II), can also be scavenged by snow (Amos et al. 2012). Data on this process has been collected through the Mercury Deposition Network (MDN) since 1996, and also through the Canadian Atmospheric Mercury Network (CAMNet) (see Fig. 2.1.3, Prestbo and Gay, 2009; Sprovieri et al. 2010). At St. Anicet, Poissant et al. (2008) measured the wet deposition flux as 0.8 ng m^{-2} hr^{-1}. At Caribou, Maine, the wet deposition flux ranged from 0.6 to 0.9 ng m^{-2} hr^{-1} between 2007 and 2015 (NADP, 2018).

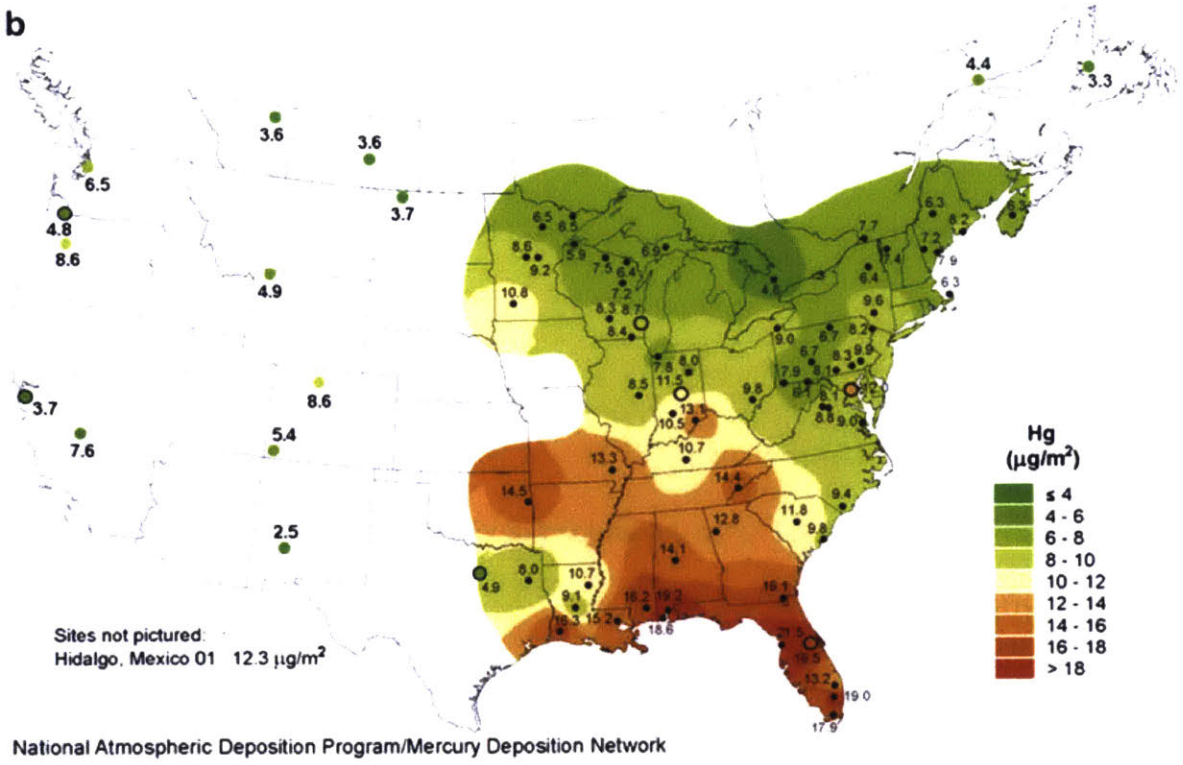

Figure 2.1.3: 2005 Hg wet deposition flux (µg/m²). Figure from Prestbo and Gay (2009). Selin and Jacob (2008) identify scavenging of free troposphere Hg(II) by deep convection in the moist Southeast as the cause of the Southeastern maximum.

Dry deposition refers to the flux of Hg to ecosystems happening at all times except periods of rainfall, and it is controlled largely by the stomatal uptake of plants (Lindberg et al. 1992). Hg(P) does not dry deposit efficiently (Amos et al. 2012). Selin and Jacob (2008) model the relative contributions of Hg(0), Hg(II), and Hg(P) to dry deposition as 60%, 37%, and 3%, respectively. Dry deposition measurements have been more difficult to constrain than wet deposition measurements due to technical limitations (Wright et al. 2016). Additionally, past attempts at measuring dry deposition have been biased toward sites that are enriched in Hg over background levels, and toward sites in the US, Europe, and East Asia (Agnan et al. 2016). Still, Wright et al. (2016) suggest that dry deposition in general is of greater total magnitude than wet deposition. At Caribou in December of 2013 and 2014, the dry deposition flux was measured at approximately 1.7 ng m^{-2} hr^{-1} (Zhang et al. 2016), while wet deposition was measured at ~0.6-0.9 ng m^{-2} hr^{-1}.

2.2. Aquatic systems

In remote aquatic systems, total Hg (inorganic Hg and MeHg) concentrations are on the order of 0.3 to 8 ng/L, while at naturally or anthropogenically enriched sites, total Hg frequently ranges from 10 to 40 ng/L and can reach up to 1000 ng/L (Wiener et al. 2003). In ten Nova Scotia lakes, O'Driscoll et al. (2017) measured average concentrations of Hg(II) in unfiltered samples at 754 pg/L with a standard deviation of 253 pg/L.

2.2.1. Methylation

It is through methylation that inorganic divalent Hg(II) is converted to the organic and bioavailable form, MeHg (Paranjape and Hall, 2017). But not all Hg(II) gets methylated (see Fig. 2.2.1). Some Hg(II) will be photoreduced to Hg(0) and proceed to volatilize (O'Driscoll et al. 2017). O'Driscoll et al. (2017) measured a mean pseudo first order

photoreduction rate of 2.07×10^{-3} per hour, with a standard deviation of 5.08×10^{-4} per hour. This photoreduction rate was balanced by a mean Hg(0) photooxidation rate measured at 2.00×10^{-3} per hour, with a standard deviation of 4.76×10^{-4} per hour (O'Driscoll et al. 2017). Although *in situ* production of MeHg often contributes substantially to total MeHg in a lake, the contribution from watershed runoff and atmospheric deposition may sometimes be greater, depending on the particular physico-chemical characteristics of the particular lake (Jonnson et al. 2014).

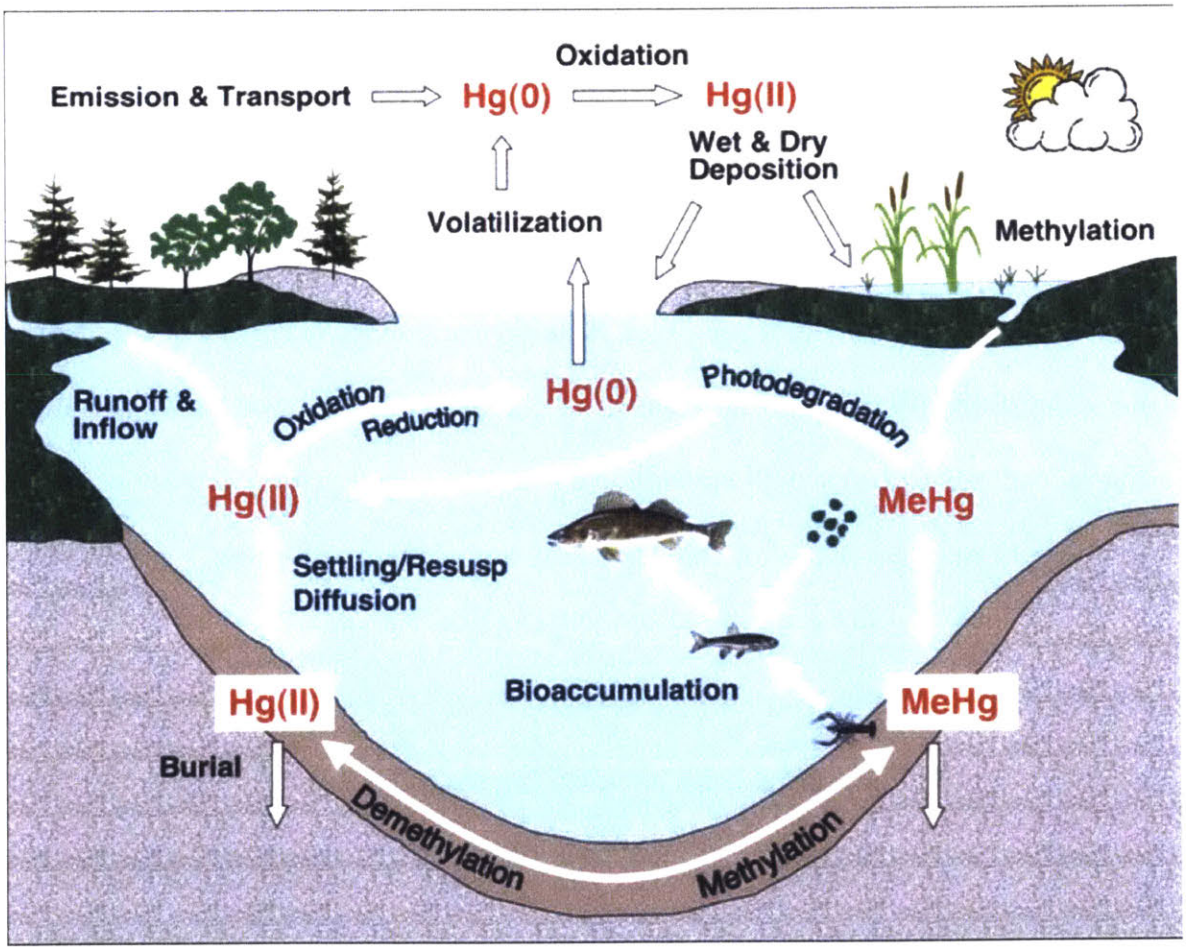

Figure 2.2.1: Aquatic Mercury Cycling. From Engstrom (2007). Once Hg(II) deposits to a lake, it may be methylated or reduced; it may sorb to a suspended particle; it may sink and settle.

There are several different possible mechanisms of methylation. In an environment rich with organic material, methylation can occur abiotically (Nagase et al. 1984). In these

saturated conditions, dissolved organic material (DOM) can donate methyl groups to Hg(II) (Ravichandran, 2004).

However, the primary mechanism of methylation is mediated by the action of sulfate-reducing bacteria (SRB) in the sediment, involving the two-gene cluster hgcAB (Parks et al. 2013). The biotic mechanism was first proposed in 1969 (Jensen & Jernelöv, 1969). Sulfate inputs tend to stimulate MeHg production by SRB (Branfireun, 1999). Outside the sediment, some other methylating bacteria may be involved (Achá et al. 2011; Gionfriddo et al. 2016). While Ullrich et al. (2001) argued that the role of methanogens in methylation was minimal, Hamelin et al. (2011) argues that methanogens may be the principal producer of MeHg in some lakes fed by rivers. At higher temperatures, bacteria are more productive in methylation (Paranjape and Hall, 2017).

Most studies of methylation in lakes have focused on its occurrence under anoxic, reducing conditions (Warner et al. 2003). But a few studies have found production occurring in oxic conditions as well. In some tropical lakes, methylating activity only occurs under oxic conditions (Correia et al. 2011). Eckley and Hintelmann (2006) found that oxic conditions may stimulate the action of bacteria that require oxygen.

Mercury interacts in a complicated way with DOM (Schartup et al. 2018). DOM can complex with Hg, inhibiting uptake by bacteria because of its large size (Ravichandran, 2004). This effect is pH dependent. At lower pH, DOM has less negative charge and is less likely to complex Hg (Barkay et al. 1997). But DOM does not always inhibit methylation. In sulfate-limited aquatic environments, DOM can stimulate microbial growth, thus indirectly increasing methylation (Watras et al. 1995). Additionally, as noted earlier, high

concentrations of DOM can increase the importance of the otherwise minimal abiotic methylation pathway (Celo et al. 2006).

Methylation can occur at a variety of locations in a lake ecosystem. Methylation tends to be at its highest levels at a lake's sediment-water interface. In a study of a seepage lake in Wisconsin, Korthals and Winfrey (1987) found minimal methylating activity in the water column, greatest activity at the surface sediment level, and decreases in sediment activity with depth. But more recent studies have found methylation occurring in the bottom of the water column. Eckley et al. (2005) measured methylating activity in the anoxic hypolimnion of two Wisconsin lakes – one seepage and one dominated by runoff from wetlands. Wetlands are an especially important location for methylation, with the periphytic biofilm on the surface of large plants being a source of production as well (Klapstein and O'Driscoll, 2017; Hamelin et al. 2015).

Actual measurements across varied aquatic ecosystems have found a large range of potential methylation rates. Hintelmann et al. (2000) measured methylation rates – first order with respect to the concentration of Hg(II) – ranging from 0.001 to 0.016 per day in the sediments of a lake in Ontario, Canada. Tjerngren et al. (2012) measured values between 0.01 up to 0.05 per day in a Swedish boreal lake. In a sub-boreal lake with chronic high sulfate inputs, Johnson et al. (2016) found methylation rates ranging from less than 0.01 to 0.33 per day.

2.2.2. Demethylation

Demethylation can occur via biotic as well as abiotic mechanisms. The same SRB which methylate Hg(II) can demethylate MeHg oxidatively, resulting in Hg(II), or

reductively, resulting in Hg(0) (Klapstein and O'Driscoll, 2017). Most biotic demethylation occurs in areas with high organic content, such as the sediment (Klapstein et al. 2017).

An abiotic mechanism of demethylation – the most important in many lake ecosystems – is photodemethylation (Klapstein and O'Driscoll, 2017). The rate of photodemethylation depends on the intensity of radiation, so the rate decreases with lake depth (Poste et al. 2015). Although UV light is more efficient than photosynthetically active radiation (PAR) in degrading MeHg, UV light attenuates more quickly with depth, so PAR is responsible for most photodemethylation (Black et al. 2012). Lakes with higher levels of DOM attenuate light more rapidly, leading to decreased rates of photodemethylation (Black et al. 2012). However, at low levels of DOM, marginal increases can actually increase the rate of photodemethylation. This is because photodemethylation depends on the absorption of radiation by DOM, followed by the production of reactive radicals (DOM*), which drive the photodemethylation pathway (Klapstein et al. 2017).

Hintelmann et al. (2000) found demethylation rates, first order with respect to the concentration of MeHg, ranging from 0.390 to 0.528 per day in the sediments of two pristine soft-water lakes in Ontario. Eckley and Hintelmann (2006) measured demethylation rates of less than 0.12 per day in the anoxic hypolimnia of five Canadian boreal and temperate lakes.

2.2.3. Bioaccumulation

The bioaccumulation of MeHg in fish can be controlled both by bottom-up processes – i.e., factors affecting the production and destruction of MeHg – as well as trophic, top-down factors relating to the structure of the food web (Rolfhus et al. 2011). Among trophic factors affecting bioaccumulation are the age, weight and trophic status of the fish, which

all positively correlate with higher bioaccumulation factors (BAFs), i.e., fish to water Hg concentration ratio (Wiener et al. 2003). Rolfhus et al. (2011) found that the largest bioaccumulation factors across a range of studies of the western Great Lakes region were between the water and seston (minute biotic and organic matter), and between the water and zooplankton, suggesting greater importance for the bottom-down factors in these lakes, like concentration of dissolved organic carbon. Within a lake, other factors being equal, fish which feed in the pelagic zone tend to have higher MeHg concentrations than fish which feed in the littoral zone (Chetelat et al. 2011). Chetelat et al. (2011) suggest that this difference is based either on variations in MeHg concentration across different lake zones, or more efficient uptake of MeHg by the pelagic food web.

Watras et al. (1998) found MeHg $\log_{10}$ BAFs in Wisconsin lake yellow perch ranging between 6 and 7, with a mean value of approximately 6.5. Hammerschmidt and Fitzgerald (2006) measured a MeHg $\log_{10}$ BAF of 6.0 for whole alewife in the marine environment of Long Island Sound.

III. RESEARCH QUESTIONS

The objective of this study is to better understand the factors that influence future (2035) concentrations of methylmercury (MeHg) in Maine freshwater fish under three different policy scenarios. We choose to focus on eastern Maine lakes because there is no known direct input of Hg from local sources. The main source of contamination is atmospheric deposition from the global Hg pool. Therefore, we can use these lakes to learn more about global processes affecting Hg transport and deposition without local interference. Additionally, we focus on lakes that are fishing sites for members of the

Wabanaki Confederacy because Wabanaki who engage in a traditional-subsistence diet are particularly vulnerable to MeHg pollution.

3.1. The Wabanaki and subsistence

The Wabanaki peoples – today comprising the Mi'kmaq, Maliseet, Penobscot, Abenaki, and Passamaquoddy bands – are a group of Algonquian-speaking tribal nations located in Maine and parts of southeastern Canada (Prins & McBride, 2007). They descend from people who have been living in Maine and Canada for over 10,000 years and who sustained themselves through gathering, hunting, fishing, and agriculture (Asch Sidell, 1999).

The diet of Maine's Wabanaki Indians was described in the early 1600s by the French Jesuit priest Biard. Biard recorded three seasonal dietary regimes among a particular Wabanaki group. From fall to late winter, the Wabanaki in southern Nova Scotia hunted inland mammals. Following the spring thaw, they would fish and catch birds. And in the early summer, they would travel to the coasts, relying on clams and marine birds for sustenance (EPA, 2009). Although Biard offers a particularly detailed account of Wabanaki subsistence in one place at one time, it would be a mistake to consider his description a prescription on what subsistence must look like. It would be a mistake, also, to think of subsistence as a relic of the 1600s. Darren Ranco writes that "a fully subsistent lifestyle and intimate knowledge of their surroundings is within the memory of today's elders or their parents" (EPA, 2009).

Within a few decades of contact with the invading Europeans in the early 1600s, over 90% of the Wabanaki population died from warfare and epidemics (smallpox, cholera, and influenza, among others) (Prins & McBride, 2007). It is likely that these epidemics

were caused by "the same forces of poverty, social stress, and environmental vulnerability that cause epidemics in all other times and places," rather than the often cited but probably specious phenomenon of Native Americans lacking genetic immunity to European diseases (Jones, 2003). In other words, the depopulation was not inevitable; it was contingent on the actions of Europeans and Native Americans in their context (Jones, 2003).

Following the American Revolution, the border between Canada and the USA was defined, splitting Wabanaki lands into two separate jurisdictions (Prins & McBride, 2007). Despite this further encroachment on the integrity of their lands, the Wabanaki have continued to cross the border in order to visit neighboring communities (Prins & McBride, 2007).

The traditional-subsistence diet is both "important to the economic well-being" of Native American communities and "is also the basis of cultural existence and survival" (EPA, 2009). Hg deposition on to Native American land from remote US and global sources impedes the healthy practice of the subsistence diet, which is central to Native cultural self-determination. Thus, this Hg deposition constitutes one further episode in the history of European and US violation of Native sovereignty (O'Neill, 2004; Ranco et al. 2011). Efforts to make the Wabanaki's desired level of fish consumption safe through regulations on Hg are a matter of environmental justice. This study investigates what factors influence MeHg concentration in the fish of tribal lakes in order to further these efforts toward reduction of MeHg in tribal lakes.

3.2. Origin and contamination of the Maine lakes

When the most recent glacial period ended, during the Younger Dryas (14,500 to 11,500 years ago), the Laurentide ice sheet, which had covered Maine, receded to the north

(EPA, 2009). This glacial erosion and accompanying deposition of silt and clay produced shallow lakes with poor drainage (EPA, 2009). Lake levels were low during this dry period, then rose at the beginning of the Holocene (11,500 years ago), before declining again from 8000 to 7200 years ago (Dieffenbacher-Krall & Nurse, 2005). Lake levels rose again, until 4800 years ago, when they declined for another 1800 years (Krall & Nurse, 2005). Once again beginning to rise after 3000 years ago, these lakes reached their current water levels within the past 600 years (Krall & Nurse, 2005).

From the 1950s to the 1980s, pulp and paper production were major industries in Maine, employing 18,000 workers. By 2017, only 4,000 workers were still employed in Maine's paper mills (WGME, 2017). These mills, as well as a chlor-alkali plant, released Hg into the Penobscot River, making it a site of legacy pollution (Sunderland et al. 2012). However, eastern Maine has not been subject to this same legacy of Hg pollution. Wet deposition measured at Mercury Deposition Network (MDN) sites in Maine and Nova Scotia ranged from 6.0 to 7.2 $\mu g/m^2/yr$ in 2003, and from 7.0 to 7.4 $\mu g/m^2/yr$ in 2009 (Sunderland et al. 2012). Of these deposition values, 71% came from global and natural sources (Sunderland et al. 2008).

In the USGS 1993 study of heavy metal pollution in Maine's lakes, 65% of the lakes sampled had at least one fish species with Hg concentrations greater than 0.43 ppm, the level established by Maine's Department of Human Services as unsafe for human consumption (Maine DEP 1995). Additionally, 9% of the lakes had fish with Hg levels greater than 1.0 ppm (Maine DEP 1995). Even more than 65% of the lakes must have exceeded the more stringent tissue-based water quality criterion of 0.3 ppm recommended by EPA.

3.3. Modeling Hg in lakes

Knightes et al. (2009) modeled responses to a hypothetical 50% decline in atmospheric deposition rates across a range of lake types. All lakes responded with a common structure: a rapid decrease in MeHg concentration of 20% to 60% over a few decades, followed by a slower decline toward steady state across several decades or centuries (Knightes et al. 2009). The lake dominated by wetland runoff inputs responded slowest, and the seepage lake, fed mostly by precipitation, responded most quickly (Knightes et al. 2009).

Instead of using a 50% hypothetical reduction, Perlinger et al. (2018) modeled reductions in MeHg concentrations in piscivorous fish in the Great Lakes region under different policy scenarios. Perlinger et al. (2018) found that after 50 years under a "*policy-in-action*" scenario, Hg concentrations in an Upper Peninsula (UP) lake would decrease by 11%, a slow change reflecting the predominance of wetlands in this area. However, in comparison to the 34% increase in deposition of Hg to the UP characteristic of the counterfactual "*failure-to-govern*" scenario, this 11% decrease appears more significant (Perlinger et al. 2018).

This study applies the same model used in Perlinger et al. 2018 and developed by Hendricks (2018). However, the model developed by Hendricks (2018) was validated for a lake in Michigan's Upper Peninsula (UP). Model outputs depend on the characteristics of the lake (e.g., depth), its watershed, and the local Hg atmospheric deposition. In order to model fish Hg concentration in Maine, the model needs to be re-evaluated and potentially re-calibrated.

IV. METHODS

Concentrations of methylmercury (MeHg) in Maine freshwater fish were modeled for the year 2035 under three different policy scenarios (see below). The lakes studied are those used by the Wabanaki tribes as a source of food, for which data have been collected in the 1993 USGS study, "Fish Tissue in Maine Lakes Contamination Report" (Maine DEP, 1995) – see map in Appendix. The three policy scenarios studied – current policy (CP), new policy (NP), and maximum feasible reduction (MFR) – represent the effect in 2035 of increasingly strict global regulations on mercury emissions. First the model was run uncalibrated, then a factorial experiment and least squares regression was performed in order to calibrate the model, and it was run again for all twenty lakes under the three policy scenarios.

4.1. Model parameterization

Figure 4.1 shows the physical and chemical processes simulated by SERAFM as implemented by Hendricks (2018). Mercury enters lakes through inflow, runoff, and deposition, and it is converted from Hg(II) to MeHg, the bioavailable species that accumulates in fish. As previously mentioned, the model developed by Hendricks (2018) was calibrated and evaluated for a lake in Michigan's Upper Peninsula (UP). In order to model fish Hg concentration in Maine, the model first needed to be re-evaluated and potentially re-calibrated.

The 1993 USGS study did not have data for every parameter required as an input to the model. Thus, we had to calculate certain parameters using other published data.

To calculate the percentage of wetland in the catchment of each lake studied, data from the National Wetlands Inventory (NWI) was superimposed on data from the

Watershed Boundary Dataset (WBD) and National Hydrography Dataset (NHD) in ArcGIS. The NWI is a dataset developed by the US Fish and Wildlife Service in 1979 that currently exists in its second implementation at a resolution of 1:24,000 (USFWS, 2016). It is a spatial representation of all the wetlands in the US. The WBD is produced by the Subcommittee on Spatial Water Data, an intergovernmental data department, and it offers hierarchically nested delineations of watershed boundaries across the US (USGS & USDA, 2013). This study made use of "subwatershed" or HU12 data, the most precisely delineated watershed boundaries currently available. The NHD results from a joint effort of EPA and USGS, and among its products is a spatial catalogue of all lakes and ponds in the US (USGS, 2010).

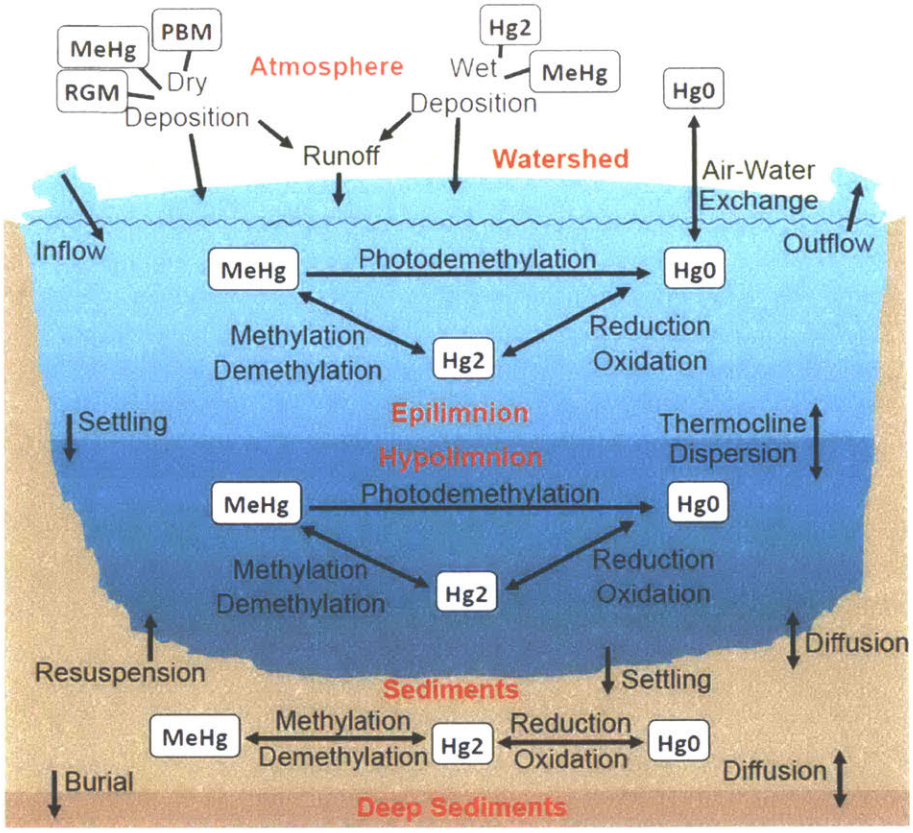

Figure 4.1: Diagram of Mercury Fate and Transport in Lakes. SERAFM simulates these physico-chemical processes to predict Hg speciation and concentration. Once Hg enters a lake from the atmosphere, the catchment, or tributaries, it can be converted to MeHg from Hg(II) by sulfate-reducing bacteria, and it will biomagnify along the food chain, expressed at increasing concentrations in organisms with increasing trophic status. SERAFM solves for an annually averaged MeHg concentration in the epilimnion, and it multiplies that value by a bioaccumulation factor (BAF) to give a distribution of MeHg concentrations in fish. From Perlinger et al. (2018).

Comparing the WBD and NHD, we located the particular subwatersheds that encompassed every lake of interest. In the one case where a lake crossed the border between two subwatersheds, those two subwatersheds were merged and treated as a single watershed. Inspection of the intersection of each subwatershed of interest with the land use data from the NWI allowed for the calculation within each subwatershed of the percentage of wetland by area. To calculate the percentage of wetland by area, we divided the area in each catchment classified as wetland by the total catchment area. Figure 4.2 shows the watershed surrounding Meddybemps Lake as an example, with wetland area in

red and the lake itself in light blue. A complete list of the lakes studied and all lake-specific parameters can be found in the appendix (Tables 7.1 and 7.2). To verify our method, we additionally calculated percentage wetland for the Adirondacks and the Upper Peninsula (UP) and compared the calculated values to those reported in Perlinger et al. (2018). Whereas Perlinger et al. (2018) reported a wetlands percentage by area of 29% and 11% in the UP and Adirondacks respectively, we found values of 30% and 6%. Part of the discrepancy between the Adirondacks values may result from our study defining the areal extent of the Adirondacks differently than how Perlinger et al. (2018) defined it.

Table 4.1. Lake Geometry values from a Lake in Michigan's Upper Peninsula. (Perlinger et al. 2018).

Parameter	Value from UP lake (Perlinger et al. 2018)	Value in 1993 USGS study?
Lake Surface Area	9,730,000 m^2	Yes
Thermocline Area	8,360,000 m^2	No
Sediment Area	8,360,000 m^2	No
Total Volume	142,483,600 m^3	Yes
Epilimnion Volume	84,600,000 m^3	No
Hypolimnion Volume	57,800,000 m^3	No
Sediment Volume	83,600 m^3	No

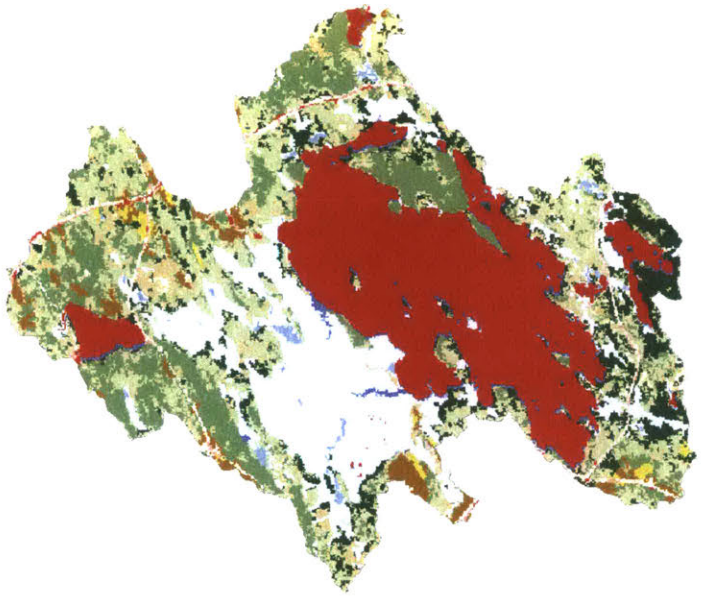

Figure 4.2: Land Use in the Meddybemps Watershed. Wetland area is in red, while the Meddybemps lake is in light blue. Wetlands are significant sites of methylmercury production and are parametrized in the model with a reduced runoff coefficient compared to other land use categories because of their capacity to trap water.

To estimate values not directly measured by the USGS 1993 study, we multiplied known values by ratios of values from Perlinger et al. (2018). Table 4.1 lists the relevant parameters from Perlinger et al. (2018) and whether or not they exist in the 1993 USGS study. Table 4.2 lists all of the ratios used based on the values in Table 4.1. We multiplied known values for our lakes by these ratios to estimate unknown values. For example, to estimate the thermocline area of a Maine lake, we multiplied the ratio of thermocline area over lake surface area from Perlinger et al. (2018) by the lake surface area recorded in the 1993 USGS study.

Table 4.2. Ratios of UP lake physical Properties. From Hendricks (2018).

Ratio	Value from UP lake (Hendricks 2018)
Thermocline Area/ Lake Surface Area	0.859
Epilimnion Volume / Total Volume	0.594
Hypolimnion Volume / Total Volume	0.406
Sediment Volume / Total Volume	0.00059

For the fluxes of Hg(0), Hg(II), and Hg(P) to the catchment by dry and wet deposition, we used values derived from the chemical transport model GEOS-Chem for the year 1993 as well as the three policy scenarios in 2035 (Pacyna et al. 2016). GEOS-Chem is a multi-media model that couples a 3D atmosphere, a 2D surface-slab ocean, and a 2D terrestrial reservoir. It uses an archive of meteorological data collected by NASA's Goddard Earth Observing System (GEOS) since 1979 to model chemical transport and transformation in the atmosphere on a global scale, at 47 different slices in the vertical, and on a 4°x5° or 2°x2.5° horizontal resolution. The model is freely accessible to the public (http://acmg.seas.harvard.edu/geos/), and it is updated frequently by users pursuing their own research. For further details, a comprehensive description of the model is available elsewhere (Travnikov et al. 2017; Horowitz et al. 2017).

The 1993 fluxes were taken from work by Muntean et al. (2014), while the 2035 policy scenarios were taken from work by Angot et al. (in prep). Hg(P) data for 1993 was not available because those simulations were performed with an older version of GEOS-Chem (v9-01-03) which did not account for particulate mercury. Thus, for 1993 Hg(P) deposition, we estimated a value based on a ratio between the mean total dry deposition and mean Hg(P) deposition over the years 2008-2014. Perlinger et al. (2018) was followed, in saying that, for Hg(II) and Hg(P), deposition directly to the lake surface would be 1/10 of deposition to the catchment because of differences in surface resistance between woods and water (Zhang et al. 2009; Angot et al. in prep). We calculated Hg(0) dry deposition to the lake surface using equations developed by Hendricks (2018) based on principles of mass transfer at the air/water interface. Since GEOS-Chem does not provide deposition fluxes for MeHg, we estimated MeHg dry and wet deposition as the multiplication of a

deposition velocity taken from Perlinger et al. (2018) by an atmospheric MeHg concentration typical for remote regions (2.00×10^{-12} mg/L) (Lindberg et al. 2007).

4.2. Model calibration

The model as implemented by Perlinger et al. (2018) was calibrated for a lake in Michigan's Upper Peninsula. To determine whether a calibration specific to Maine's environment was required, we first used the same values used by Perlinger et al. (2018) for those environmental parameters that there was not data for in the context of Maine, such as the methylation rate. We only changed lake-specific parameters (see Table 5.4) like percentage of wetlands in the catchment and lake surface area, for which we had data. In other words, in our preliminary run, we did not calibrate the model to Maine's physico-chemical conditions. These uncalibrated model runs were compared to the mercury concentrations reported in the USGS 1993 study (see Section V) and it was decided to re-calibrate the model.

To better calibrate the model for the Maine lakes, we first identified key parameters, and then optimized their values to match observations through a factorial experiment. One-at-a-time sensitivity analyses (OATSA) of all the parameters in SERAFM, performed just on Portland Lake, allowed for the identification of those parameters for which an uncertainty in their value would have the greatest effect on fish Hg concentration. Each parameter was perturbed by ±25% of its initial value, as well as perturbed by ±two orders of magnitude. The resulting change in piscivore median methylmercury concentration demonstrated the sensitivity of each parameter. A 25% perturbation was chosen because it is a relatively small perturbation, likely to produce a linear response. Sensitivity analyses tend to assume linearity. The two orders of magnitude perturbation was chosen to see the extent of

nonlinearity in the model: will the model still approximate linearity given extreme changes in parameter values? Any change in MeHg concentration below a threshold 0.01% was recorded as not exhibiting an effect. A list of parameter values as reported in the literature was also compiled, in order to get a sense for how certain or uncertain the particular value for each parameter was.

The factorial experiment was not simply performed on the most sensitive parameters. (See the Engineering Statistics Handbook for a broader discussion of factorial experiments (https://www.itl.nist.gov/div898/handbook/pri/section3/pri333.htm).) We investigated the sensitivities in the context of their uncertainties in order to choose parameters on which to perform a factorial experiment. In other words, those parameters whose values were well-constrained through measurements were not chosen for the experiment. The parameters chosen were both those that simulated MeHg concentrations were sensitive to, and those whose values were relatively uncertain. Namely, we chose to perform the factorial experiment on (1) the volumetric outflow rate from the lake, (2) the particle settling velocity, (3) the particle burial velocity, and (4) the partitioning coefficient for Hg(II) to biotic solids.

We sampled five points evenly spaced within a distribution of values for each parameter and ran the model for every possible combination of the five points over the four parameters, which is equivalent to 5^4, or 625, combinations. The distributions chosen were based on measured values from the literature, but expanded to better understand system behavior at extremes. Then a least squares regression was performed in order to find the set of parameters which yielded the minimum distance between the modeled and measured values across two different (but overlapping) sets of ten of the lakes. Ten lakes

were randomly chosen from the set of twenty (see appendix Table 7.1). The square of the difference between the measured whole (rather than fillet, following Hammerschmidt and Fitzgerald (2006)) piscivore MeHg concentration and the modeled median piscivore MeHg concentration (both with units of mg/L, wet weight) from each combination of parameters used in the factorial experiment were summed over the ten lakes. The smallest sum among these 625 sums was chosen as representing the optimal set of parameters for each of the two sets of ten lakes. The two sets of lakes returned different optimal parameters. The set of optimal parameters which had the smallest least squares distance between the modeled and measured results over the training set was chosen for implementation in the model. In order to ensure that the model was functioning properly, the optimization was also performed over all the lakes individually. Nearly perfect matches were expected and observed. Finally, the model was run again, this time with the calibrated parameters on all twenty of the lakes. Once again, we compared these calibrated model values to the values from the 1993 study.

4.3. Evaluation of policy scenarios

We ran the calibrated model under three different policy scenarios taken from Pacyna et al. (2016): current policy (CP), new policy (NP), and maximum feasible reduction (MFR), for all twenty lakes. Each policy reflects different levels of global mercury emissions. In every scenario, global population growth by 1.7 billion people, and Gross Domestic Product (GDP) growth by 3.2% per year are projected against differing levels of Hg regulation (Pacyna et al. 2016). The CP scenario represents the fulfillment of all regulations set to be implemented in 2010, including the implementation of air pollution control devices and the switch to low-carbon fuels (Pacyna et al. 2016). The NP scenario

projects the use of more advanced waste practices, more reductions of greenhouse gas emissions, and 70% reductions in Hg in products as compared to 2010, in accordance with the Minamata convention (Pacyna et al. 2016). Finally, the MFR scenario imagines mercury levels if the maximum possible reduction in each sector is implemented without regard for other constraints (Pacyna et al. 2016). Figure 4.3 demonstrates global mercury emissions by sector under these three policy scenarios as compared to 2010 emissions. These different scenarios translate into different fluxes of Hg deposition to the watershed and catchment.

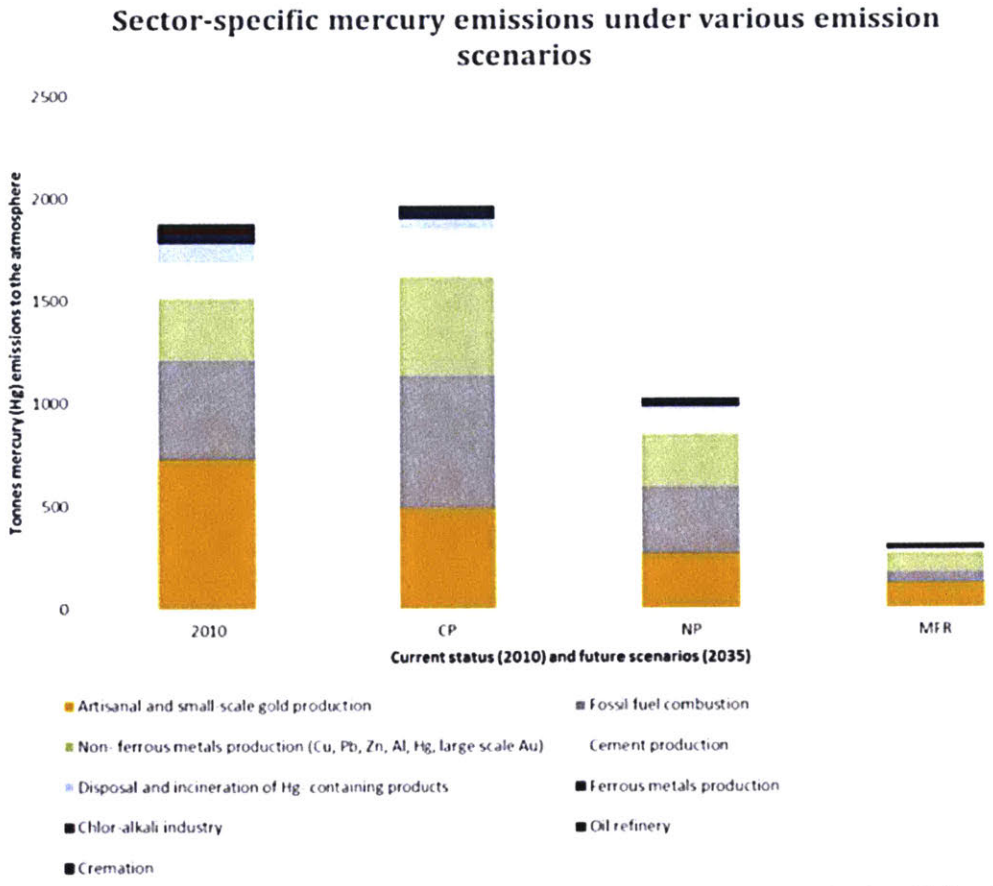

Figure 4.3: Emissions Scenarios by Sector. A business as usual scenario (CP) will lead to increased total Hg emissions and depositions in 2035. Stricter regulations will reduce emissions. Figure from Pacyna et al. (2016).

V. RESULTS

5.1. Wetland area

Wetland areas in the catchment of each lake are shown in Table 5.1. The values ranged from a minimum of 3.74% in Chase's catchment, to a maximum of 30.31% in Cross's catchment. The mean value over all twenty lakes was 14.28%.

Table 5.1. Wetland Area from National Wetland Inventory

Lake	Wetland Percent by Area
Brackett	5.31
Bradbury	9.71
Chandler	10.89
Chase	3.74
Cross	30.31
Eagle	11.22
Grand	5.75
Keene	10.00
Lambert	16.53
Machias	17.85
Meddybemps	19.28
Molunkus	13.72
Monson	16.02
Orange	19.16
Pennington	18.38
Portland	25.77
Pleasant	19.28
Sly Brook	7.66
Togue	4.07
Umcolcus	20.86

5.2. GEOS-Chem deposition fluxes

Table 5.2 shows the deposition fluxes produced by Muntean et al. (2014) and Angot et al. (in prep) for the year 1993, and the 2035 scenarios CP, NP, and MFR taken from Pacyna et al. (2016). For every category of dry deposition, the highest values among the four conditions modeled occurred for CP. Total wet deposition for 1993 was greater than that for the CP scenario. Of the three 2035 scenarios, MFR demonstrated the lowest Hg levels for dry and wet deposition, followed by NP. The MFR scenario showed a reduction in

total dry deposition of 23.35% and a reduction in total wet deposition of 26.47% compared to the CP scenario.

Table 5.2. Hg deposition flux values from GEOS-Chem. 1993 values from Muntean et al. (2014). All other values from Angot et al. (in prep). Hg(P) for 1993 was calculated differently (See Section 3.1)

	unit	1993	2035 CP	2035 NP	2035 MFR
Total Deposition	$\mu g/m^2/year$	19.31	21.17	18.41	16.01
Total Dry Deposition	$\mu g/m^2/year$	11.80	14.22	12.51	10.90
Dry Hg(0) Deposition	$\mu g/m^2/year$	10.17	11.4	10.05	8.82
Dry Hg(II) Deposition	$\mu g/m^2/year$	1.63	2.69	2.35	1.99
Dry Hg(P) Deposition	$\mu g/m^2/year$	0.08*	0.12	0.11	0.09
Total Wet Deposition	$\mu g/m^2/year$	7.51	6.95	5.90	5.11

5.3. Uncalibrated results

The uncalibrated model runs did not fit well for each lake. The total distance between the modeled results and the measured whole fish results, calculated as the sum of the squared distance between the modeled and measured median piscivore MeHg concentration for each lake, was equal to 3.69. For just the 10 lakes that were later calibrated, the squared distance was equal to 1.71. Although there was some overlap between the distributions of the modeled and measured fish concentrations, as shown in Figure 5.1, the median modeled concentration fell short of the median measured whole fish MeHg value. The median measured piscivore MeHg concentration was 0.41 mg/L WW, while the median of all the simulated median piscivore MeHg concentrations was 0.22 mg/L WW, a value 46% lower. For the modeled concentrations, 0.41 mg/L WW occurred at the 72^{nd} percentile, while for the measured concentrations, 0.21 mg/L WW occurred at the 5^{th} percentile.

The median BAF value is normalized for a fish of 42 cm, which is about the same size as most of the fish in the 1993 USGS study, as can be seen in Table 5.3. The largest discrepancies are between model values and measured values of yellow and white perch. For these two species, the model might be expected to overestimate MeHg concentrations, since in general larger fish are older fish who have had more time to bioaccumulate MeHg. It should be noted that the model predicts concentrations for fish with a distribution of sizes about an invariant mean (Perlinger et al. 2018).

Table 5.3. Fish Species and Sizes. Data from Maine DEP (1995).

Fish Species	Characteristic Length (in cm)
Lake Trout	40.64-55.88
Cusk/Burbot	35.56-50.8
Landlocked Salmon	35.56-45.72
Brown Trout	30.48-45.72
Brook Trout	20.32-35.56
Smallmouth Bass	25.40-40.64
Largemouth Bass	30.48-40.64
Chain Pickerel	35.56-55.88
Yellow Perch	20.32-30.48
White Perch	20.32-30.48

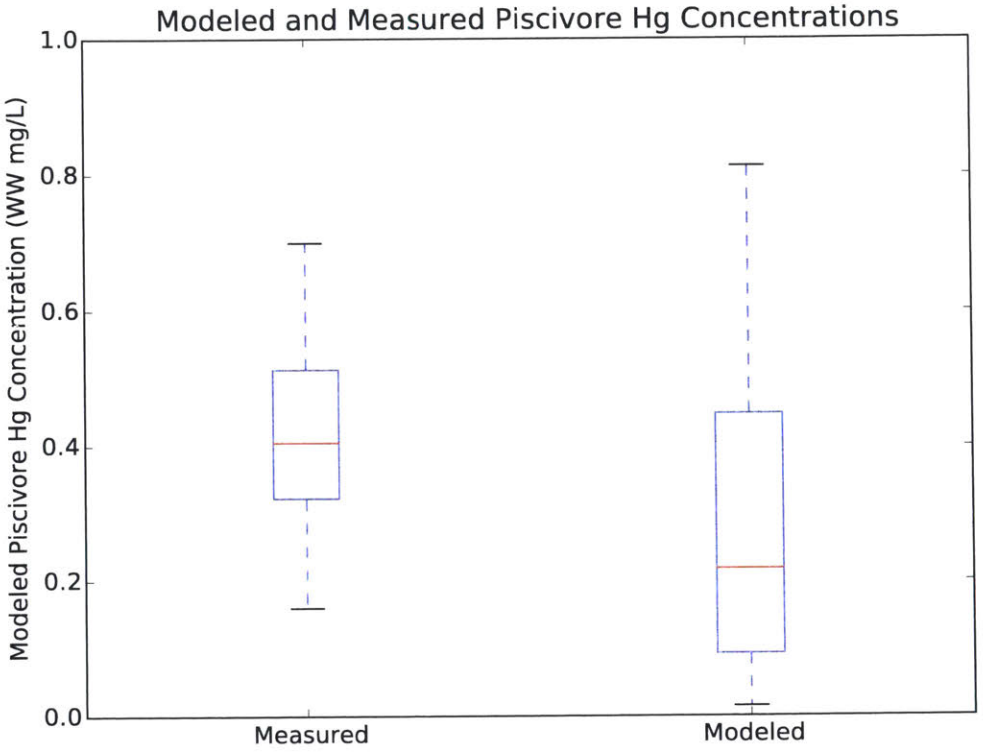

Figure 5.1: Boxplot of Modeled and Measured MeHg Concentrations. In red is the median value of each dataset, while the 25th and 75th percentiles are shown in blue below and above the median. The black lines represent the 5th and 95th percentiles. Outliers (below and above 5th and 95th percentiles) are omitted. The distribution of modeled median MeHg concentrations for piscivorous fish in all twenty lakes were plotted against the distribution of measured values. Modeled values overlapped with measured values but in general were underestimated.

5.4. Sensitivity analyses

The results of the sensitivity analyses performed on every parameter in the lake model following 25% and two orders of magnitude change in parameter value up and down are presented in Tables 5.4, 5.5, 5.6, and 5.7. Following Hendricks (2018), for each parameter, the model was run for 10 years in order to reach a steady state MeHg concentration. If a parameter perturbation produced a change in MeHg of less than 0.01%, the table records no change.

The parameters that produced the largest percent change in MeHg fish tissue concentration after a 25% variation are the settling velocity, followed by the methylation rate constant in the water column, followed by thermocline area. The parameters that produced the largest percent change after two orders variation were watershed area, followed by Hg concentration in lake inflow, followed by the volumetric inflow rate. Those parameters that exhibited no effect on MeHg concentrations following either variation were MeHg dry deposition velocity to the catchment, photosynthetically active radiation (PAR) in the hypolimnion and sediment, sediment bulk density, and the MeHg aqueous diffusivity coefficient.

Smaller perturbations in parameter value ought to approximate linear response more accurately than large perturbations. The 25% variation provoked a perfectly linear response for many of the parameters, including resuspension velocity, Hg(II) abiotic partitioning coefficient, and deep sediment porosity; for all of these parameters, a 25% variation in magnitude in either direction produced a resulting MeHg concentration percent change of the same magnitude. No two-order perturbation induced a perfectly linear response from the model, though the solids ratio in epilimnion and the volumetric outflow rate came close to inducing such a response.

Table 5.4. Sensitivity Analyses for Lake Morphology Parameters.

Parameter	Change after 25% increase	Change after 25% decrease	Change after 2 order increase	Change after 2 order decrease
Epilimnion Volume	7.52% increase	8.76% decrease	117.70% increase	46.52% decrease
Deep Sediment Porosity	0.05% decrease	0.05% increase	9.00% decrease	0.21% increase
Deep Sediment	0.05% increase	4.58% decrease	0.23% increase	10.24% decrease

Thickness				
Hypolimnion Volume	3.96% increase	4.14% decrease	133.64% increase	17.04% decrease
Lake Surface Area	0.76% decrease	1.08% increase	323.46% increase	7.45% increase
Sediment Area	1.13% increase	1.35% decrease	80.77% increase	37.24% decrease
Sediment Bulk Density	No change	No change	No change	No change
Sediment Volume	1.05% decrease	1.57% increase	15.93% decrease	56.65% increase
Surface Sediment Porosity	4.47% increase	4.58% decrease	380.33% increase	18.84% decrease
Surface Sediment Thickness	3.65% decrease	5.93% increase	18.84% decrease	380.32% increase
Thermocline Area	17.18% decrease;	25.52% increase	99.73% decrease	3819.81% increase
Volumetric Inflow Rate	7.82% increase	7.82% decrease	3098.21% increase	30.98% decrease
Volumetric Outflow Rate	11.54% decrease	14.50% increase	99.17% decrease	92.39% increase
Watershed Area	15.06% increase	15.06% decrease	5965.47% increase	59.65% decrease
Wetland Area Fraction	0.15% increase	0.14% decrease	57.52% increase	0.57% decrease

Table 5.5. Sensitivity Analyses for Hg Concentrations.

Parameter	**Change after 25% increase**	**Change after 25% decrease**	**Change after 2 order increase**	**Change after 2 order decrease**
Hg Concentration in Lake Inflow	8.44% increase	8.44% decrease	3341.58% increase	33.42% decrease
Hg(0)	0.02%	0.01%	5.76% increase	0.06% decrease

Concentration in Sediment	increase	decrease		
Hg(0) Gaseous Concentration	No change	No change	0.77% increase	0.01% decrease
Hg(II) Concentration in Sediment	0.01% increase	0.02% decrease	6.19% increase	0.06% decrease
MeHg Concentration in Sediment	0.01% increase	No change	2.20% increase	0.02% decrease
MeHg Fraction of Wet Deposition	1.30% increase	1.30% decrease	513.50% increase	5.13% decrease
MeHg from Wetlands Runoff Coefficient	3.49% increase	0.35% decrease;	137.69% increase	1.38% decrease
MeHg Gaseous Concentration	0.78% increase	0.77% decrease	307.12% increase	3.07% decrease

Table 5.6. Sensitivity Analyses for Hg Rates and Processes Parameters.

Parameter	**Change after 25% increase**	**Change after 25% decrease**	**Change after 2 order increase**	**Change after 2 order decrease**
Burial Velocity	8.9% decrease	13.24% increase	60.32% decrease	145.1% increase
Demethylation Rate Constant in the Sediment	0.98% decrease	1.60% increase	5.14% decrease	71.77% increase
Demethylation Rate Constant in the Water Column	8.93% decrease	11.13% increase	97.00% decrease	71.18% increase
General Runoff Coefficient	0.18% increase	0.17% decrease	69.62% increase	0.70% decrease
Hg(0) Abiotic Partitioning Coefficient	No change	No change	0.03% increase	3.15% decrease
Hg(0) Biotic	1.19%	1.28% increase	45.56% decrease	5.81% increase

Partitioning Coefficient	decrease			
Hg(0) DOC Partitioning Coefficient	0.06% decrease	0.07% increase	17.15% decrease	0.25% increase
Hg(0) Sediment Phase Partitioning Coefficient	0.21% decrease	0.29% increase	1.5% decrease	2.06% increase
Hg(II) Abiotic Partitioning Coefficient	0.34% decrease	0.34% increase	50.22% decrease	1.37% increase
Hg(II) Biotic Partitioning Coefficient	16.28% decrease	25.43% increase	89.97% decrease	820.74% increase
Hg(II) DOC Partitioning Coefficient	0.41% decrease	0.40% increase	60.38% decrease	1.6% increase
Hg(II) Sediment Partitioning Coefficient	2.66% decrease	4.33% increase	13.77% decrease	350.34% increase
MeHg Aqueous Diffusivity Coefficient	No change	No change	No change	No change
MeHg Biotic Partitioning Coefficient	5.04% increase	6.64% decrease	115.66% increase	73.80% decrease
MeHg Dry Deposition Velocity to Catchment	No change	No change	No change	No change
MeHg Dry Deposition Velocity to Lake Surface	0.01% increase	No change	1.52% increase	0.02% decrease
MeHg Sediment Partitioning Coefficient	0.07% increase	0.06% decrease	33.31% decrease	84.07% increase
Methylation Rate Constant in the Sediment	No change	No change	1.50% increase	No change
Methylation Rate Constant in the Water Column	21.54% increase	22.01% decrease	688% increase	89.66% decrease

Oxidation Rate Constant	0.10% increase	0.17% decrease	0.30% increase	31% decrease
Photodemethylation Rate Constant	0.01% decrease	No change	2.09% decrease	0.02% increase
Reduction Rate Constant	0.03% increase	No change	6.4% increase	0.44% decrease
Resuspension Velocity	4.27% increase	4.27% decrease	506.37% increase	17.27% decrease
Settling Velocity	19.78% decrease	30.69% increase	96.96% decrease	497% increase
Thermocline Dispersion Velocity	1.13% increase	1.65% decrease	7.36% increase	24.25% decrease
Wind Speed at 10 meters	No change	No change	7.90% decrease	0.01% increase

Table 5.7. Sensitivity Analyses for Lake Chemistry Parameters.

Parameter	**Change after 25% increase**	**Change after 25% decrease**	**Change after 2 order increase**	**Change after 2 order decrease**
Abiotic Solids Concentration in Epilimnion	0.10% decrease	0.154% increase	20.99% decrease	0.54% increase
Abiotic Solids Concentration in Hypolimnion	0.14% decrease	0.15% increase	19.25% decrease	0.59% increase
Abiotic Solids Concentration in Sediment	No change	No change	0.01% decrease	No change
Biotic Solids Concentration in Epilimnion	5.36% decrease	6.23% increase	50.45% decrease	16.53% decrease
Biotic Solids Concentration in Hypolimnion	7.92% decrease	12.27% increase	44.07% decrease	269.40% increase
Biotic Solids Concentration in Sediment	No change	No change	0.35% decrease	No change

Epilimnion DOC	0.44% decrease	0.45% increase	39.34% decrease	1.83% increase
Epilimnion Temperature	14.99% increase	13.15% decrease	234.40% increase	40.68% decrease
Hypolimnion DOC	1.13% increase	1.14% decrease	178.57% increase	4.61% decrease
Hypolimnion Temperature	1.01% increase	0.82% decrease	36.32% increase	2.15% decrease
PAR in Epilimnion	0.01% decrease	No change	2.79% decrease	0.03% increase
PAR in Hypolimnion	No change	No change	No change	No change
PAR in Sediment	No change	No change	No change	No change
Solids Ratio in Epilimnion	5.02% decrease	6.29% increase	49.92% decrease	42.17% increase
Solids Ratio in Deep Sediment	No change	No change	21.23% increase	0.21% decrease
Solids Ratio in Hypolimnion	2.70% increase	2.83% decrease	3.75% increase	12.20% decrease
Solids Ratio in Sediment	2.54% decrease	4.18% increase	237.95% increase	4.83% decrease

5.5. Data constraints on parameters

Table 5.8 lists values found in the literature associated with parameters from the SERAFM model.

For surface sediment thickness, Zhu et al.'s (2017) value of 0.01 m comes from the Hg-contaminated Xiaxi river in China, while the Sando's (1994) value comes from Lake Byron in South Dakota. Lake Byron formed through the recession of glaciers at the end of

the last glacial period, in the same way that Maine's lakes formed. Sando (1994) also records a value of 3.05 m for the thickness of the deep sediment. The Hg Report's surface sediment thickness value of 0.02 is suggested as a typical surface sediment thickness for a lake in the eastern US.

In Zhang's (2016) study of Lake Michigan, surface sediment porosity values were collected that ranged from 0.718 to 0.979. The value from the model as recorded in Hendricks (2018) of 0.9 fits comfortably within this range, which stands to reason as Torch Lake, the lake studied by Hendricks (2018), comes from the geographically similar region of Michigan's Upper Peninsula.

Zhang (2016) recorded a range of local sediment bulk densities in Lake Michigan from 5.3×10^4 to 6.9×10^5, with the Hendricks (2018) value once again fitting within that range. The value of 1.4×10^6 from Lyon et al. (1997) was not a measurement, but a value used in their calculation of soil-water and benthic sediment partition coefficients for Hg(II) and MeHg.

The Mercury Study Report to Congress (1997) suggested a value of 1.2 mg/L as reasonable for a generic eastern US lake's abiotic solids concentration in the epilimnion.

In the Zhu et al. (2017) study of Hg contamination in the Xiaxi River, as well as in the Hendricks (2018) model calibration for Michigan's Torch Lake, a partition coefficient of 0 L/mg was used for Hg(0)'s sorption to abiotic and biotic solids, and for its partitioning to the sediment phase. This value is premised on the fact that neutral species have poor sorption capacity.

Ambrose et al. (2005) uses a Hg(II) DOC partitioning coefficient of 0.02 L/mg in their study of Hg deposition into the Ochlokonee River watershed in Georgia, an order of

magnitude smaller than the value 0.25 used by Hendricks (2018) for Torch Lake. The values from Ambrose et al. (2005) and Hendricks (2018) for MeHg's DOC partition coefficient of 0.2 and 0.1 respectively, are more similar to each other.

The Hg(II) sediment partitioning coefficients calculated by Lyon et al. (1997) ranged from 0.0033 to 0.06 L/mg, while Allison and Allison (2005) calculated a range of values from 0.006309 to 1 L/mg, with a median value of 0.0794 L/mg. Hendricks (2018) uses this median value from Allison and Allison (2005) as their value. Hammerschmidt (2004) records Hg(II) sediment partitioning coefficients in Long Island Sound ranging from 0.002691 to 0.057543 L/mg. All four of these studies report MeHg sediment partitioning coefficients about one to two orders of magnitude lower than the Hg(II) values.

Kuss et al. (2009) uses molecular dynamics simulation to calculate elemental mercury's diffusivity coefficient and finds a range of values roughly 3x as large as the value used by Hendricks (2018) for the model of Torch Lake.

Prestbo and Gay (2009) use Hg wet deposition values recorded by the North American Mercury Deposition Network (MDN) to calculate a range of total Hg atmospheric concentration from 3×10^{-6} to 5×10^{-6} mg/L. Agnan et al. (2016) records values just for Hg(0) concentration three orders smaller in their meta-analysis of 132 studies, with 1290 reported fluxes from over 200,000 measurements. The Hg(0) concentration used by Hendricks (2018) falls within the range of smaller values reported by Agnan et al. (2016).

Poissant et al. (2005) recorded Hg(II) concentrations in the atmosphere of southern Québec of $3 \pm 11 \times 10^{-12}$ mg/L, with the value from Hendricks (2018) of 1.17×10^{-11} falling at the upper edge of this range. Poissant et al. (2005) recorded Hg(P) concentrations at an

order of magnitude greater than Hg(II) values, and Hendricks (2018) uses a Hg(P) concentration which falls at the lower end of the range recorded by Poissant et al. (2005).

The bioaccumulation factors recorded by Watras et al. (1998) in 15 Wisconsin lakes for perch fish, and the value recorded by Hammerschmidt and Fitzgerald (2006) in Long Island Sound for alewives were all on the order of 10^6 - 10^7 L/kg, values which accord with the ones used by Hendricks (2018) for median mixed feeder and median piscivore MeHg BAF, 1.6×10^6 and 6.8×10^6, respectively. The 4.25x larger piscivore BAF is in agreement with the principle of bioconcentration: organisms of higher trophic status will have greater MeHg concentrations.

O'Driscoll (2017) records photo-oxidation and photo-reduction rate constants in samples from Kejimkujik National Park, Nova Scotia of roughly 0.03 to 0.08 day^{-1} for both processes. These values are three orders of magnitude lower than the one used by Hendricks (2018) for oxidation, and one order lower than the value used for reduction, both of which were calculated specifically for Torch Lake. One explanation for this discrepancy may be that other mechanisms for oxidation and reduction outside light action predominate in Torch Lake as compared to Kejimkujik.

In the review of literature on methylation and demethylation in Paranjape and Hall (2017), a range of values for the methylation rate constant in the sediment is recorded as 0.001 to 0.016 day^{-1} for Ontario, Canada. Paranjape and Hall (2017) also record values for methylation in the water column ranging from 0.0014 to 0.01 day^{-1}, taken from boreal Sweden. While Paranjape and Hall (2017) note methylation values as high as 0.12 day^{-1}, these values come from the significantly different climate of the Florida Everglades and thus were excluded from this survey.

For demethylation in the sediments and water column, Paranjape and Hall (2017) record ranges from 0.016 – 0.022 and 0 - 0.007 day^{-1}, respectively. Once again, larger values, this time from the water column in the High Arctic, were excluded due to climatic differences.

Table 5.8. Survey of Parameter Values from Literature

Parameter	Units	Value from Model (Hendricks 2018)	Value from Literature	References
Surface Sediment Thickness	m	0.005	0.01; 0.366; 0.02	Zhu et al. (2017); Sando (1994); Hg Study Report to Congress
Deep Sediment Thickness	m	0.1	3.05	Sando (1994)
Surface Sediment Porosity	unit-less	0.9	0.718 - 0.979	Zhang (2016)
Sediment Bulk Density	mg/L	1×10^5	$5.3 \times 10^4 - 6.9 \times 10^5$; 1.4×10^6	Zhang (2016); Lyon et al. (1997)
Abiotic Solids Concentration in Epilimnion	mg/L	0.3	1.2	Hg Study Report to Congress
Hg(0) Abiotic Partitioning Coefficient	L/mg	0	0	Zhu et al. (2017)
Hg(0) Biotic Partitioning Coefficient	L/mg	0	0	Zhu et al. (2017)
Hg(2) DOC Partitioning Coefficient	L/mg	0.25	0.02	Ambrose et al. (2005)
MeHg DOC Partitioning Coefficient	L/mg	0.1	0.2	Ambrose et al. (2005)
Hg(0) Sediment Partitioning	L/mg	0	0	Zhu et al. (2017)

Coefficient				
Hg(2) Sediment Partitioning Coefficient	L/mg	0.0794	0.0033 - 0.06; 0.006309 - 1, mdn: 0.079432; 0.002691 - 0.057543	Lyon et al. (1997); Allison and Allison (2005); Hammerschmidt (2004)
MeHg Sediment Partitioning Coefficient	L/mg	0.00794	2×10^{-5} - 0.0067; 6.31×10^{-4} - 0.1, mdn: 0.003981; 6.0255×10^{-5} - 0.001023	Lyon et al. (1997); Allison and Allison (2005); Hammerschmidt (2004)
Hg(0) Aqueous Diffusivity Coefficient	m^2/ day	5.55×10^{-5}	1.44288×10^{-4} - 1.62432×10^{-4}, from 20°C to 25°C	Kuss et al. (2009)
Hg(0) gaseous concentration	mg/L	1.42×10^{-9}	$3\text{-}5 \times 10^{-6}$; $1.0 - 1.7 \times 10^{-9}$	Prestbo and Gay (2009); Agnan et al. (2016)
Hg(2) Gaseous Concentration	mg/L	1.17×10^{-11}	$3 \pm 1 \times 10^{-12}$	Poissant et al. (2005)
Hg(P) Gaseous Concentration	mg/L	1.08×10^{-11}	$2.6 \pm 5.4 \times 10^{-11}$	Poissant et al. (2005)
50th Percentile Bioaccumulation Factor for Mixed Feeder Fish	L/kg	1.6×10^{6}	10^{6} - 10^{7}, mean $10^{6.5}$; 10^{6}	Watras et al. (1998); Hammerschmidt and Fitzgerald (2006)
50th Percentile Bioaccumulation Factor for Piscivores	L/kg	6.8×10^{6}		
Oxidation Rate at Reference T	1/day	10	0.034 - 0.073	O'Driscoll (2017)
Reduction Rate at Reference T	1/day	0.5	0.039 – 0.08	O'Driscoll (2017)
Methylation Rate in Water Column at Reference T	1/day	0.1	0.0014 - 0.01	Paranjape and Hall (2017)
Methylation Rate in Sediment at Reference T	1/day	0.0007	0.001 - 0.016	Paranjape and Hall (2017)
Demethylation	1/day	1	Negligible - 0.007	Paranjape and

Rate in Water Column at Reference T				Hall (2017)
Demethylation Rate in Sediment at Reference T	1/day	100	0.016 - 0.022	Paranjape and Hall (2017)
Fraction of MeHg in Wet Deposition	unit-less	0.015	<6%	Hall et al. (2005)

5.6. Calibration

A calibration performed against four parameters of interest yielded the values shown in Table 5.9.

Table 5.9. Calibrated Values from Factorial Experiment.

Parameter	Calibrated Value
Volumetric Outflow Rate	100,000 m^3 day^{-1}
Settling Velocity	1.2 m day^{-1}
Burial Velocity	5.75×10^{-6} m day^{-1}
Hg(II) Biotic Solids Partitioning Coefficient	0.55 L mg^{-1}

5.7. Calibrated results

The calibrated results, shown in Figure 5.2, showed a moderate improvement in accuracy compared to the uncalibrated results. The total distance between the measured and calibrated results was 2.56, compared to a value for the uncalibrated results of 3.69. For just the 10 lakes chosen as the training set for the calibration, the squared distance was 1.17 compared to a value of 1.71 for the uncalibrated results. The optimal parameters from the second training set returned a square distance of 1.31 over the training set, a value 12% larger than the distance for the other training set, but still 23% smaller than the uncalibrated distance.

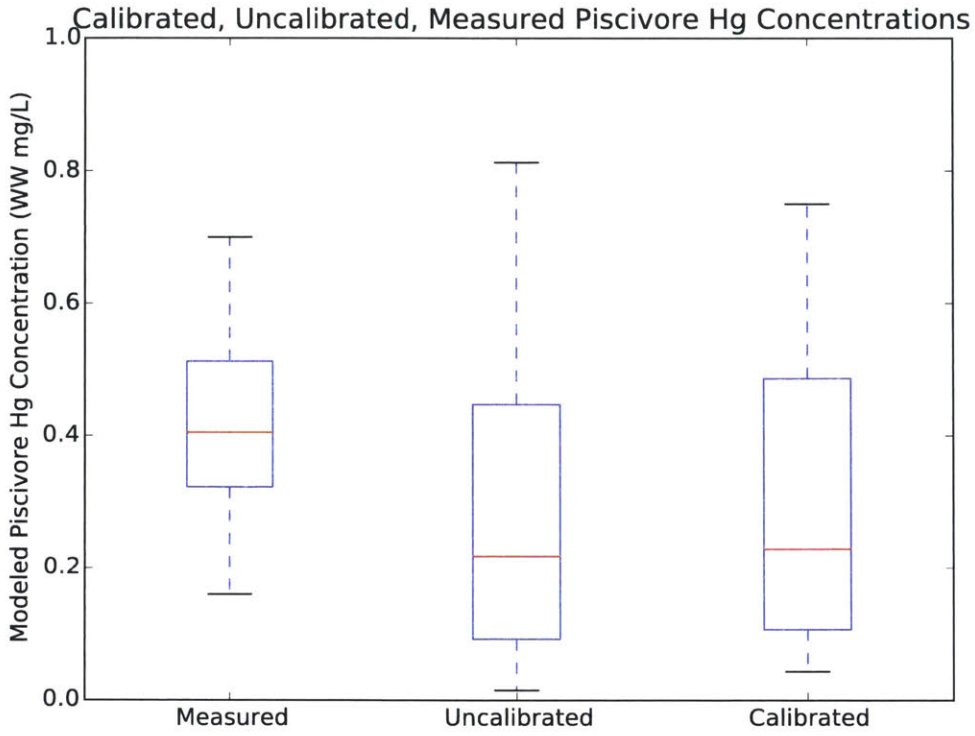

Figure 5.2: Boxplot of Modeled (calibrated and uncalibrated) and Measured MeHg Concentrations. Outliers excluded. Following calibration, the modeled median MeHg concentrations in piscivores still tend lower than the values measured in Maine DEP (1995).

5.8. Projections to 2035

The calibrated model was used to project Hg concentrations for the year 2035 under three different policy scenarios, each representing a different level of global Hg regulation as reflected in different Hg atmospheric deposition levels. Table 5.10 shows the percent reduction in MeHg fish concentrations projected by the calibrated model for the three scenarios as compared to 1993 levels. On average, MeHg concentrations in the CP scenario demonstrated a reduction of 2.61%, the NP scenario demonstrated a reduction of 11.55%, and the MFR scenario a reduction of 18.51%. For the CP scenario, Chase showed the least reduction – it actually increased by 2.45% - and Sly Brook the most. For the NP scenario,

Grand showed the least reduction and Sly Brook the most. For the MFR scenario, Grand showed the least reduction and Sly Brook the most.

Table 5.10. Percent Reduction for Each Scenario in all Lakes. A + indicates a percent increase.

Lake	CP vs. 1993	NP vs. 1993	MFR vs. 1993
Brackett	0.79%	10.26%	17.85%
Bradbury	3.46%	12.40%	19.26%
Chandler	3.21%	11.81%	18.42%
Chase	+2.45%	8.56%	17.75%
Cross	3.84%	12.95%	19.92%
Eagle	4.17%	13.24%	20.14%
Grand	+1.41%	5.74%	11.70%
Keene	2.27%	11.26%	18.30%
Lambert	3.59%	12.93%	20.12%
Machias	3.99%	13.02%	19.91%
Meddybemps	1.54%	11.51%	19.42%
Molunkus	1.75%	11.62%	19.42%
Monson	2.25%	7.84%	12.11%
Orange	3.01%	11.52%	18.08%
Pennington	2.83%	12.37%	19.79%
Portland	4.22%	13.38%	20.34%
Pleasant	2.59%	12.14%	19.59%
Sly Brook	4.65%	13.60%	20.35%
Togue	3.84%	12.27%	18.68%
Umcolcus	4.01%	12.52%	18.98%

VI. DISCUSSION

6.1. Optimal parameter values

Table 5.8 records the following optimized parameter values from the factorial experiment: a volumetric flow rate of 100,000 m^3 day^{-1}, a settling velocity of 1.2 m day^{-1}, a 5.75×10^{-6} m day^{-1}, and a Hg(II) Biotic Solids Partitioning Coefficient of 0.55 L mg^{-1}. The increase in accuracy from the model parameters can be represented as the percent decrease in square distance between modeled and measured results. For all twenty lakes, this percent decrease equals 30.57%. For just the training set, this percent decrease equals 31.95%. It stands to reason that the lakes the model was trained on should demonstrate a

greater accuracy as measured by a greater percent reduction, as compared to the entire set of lakes. The fact that the two percent reductions are as similar as they are suggests that the improvement lake by lake between the uncalibrated and calibrated model may have been quite regular.

For the four parameters chosen, three (settling velocity, burial velocity, and the Hg(II) biotic solids partitioning coefficient) govern the transport of Hg between different phases and lake compartments. The fourth, volumetric outflow rate, is a lake-specific parameter for which I did not have data at first. Although we recently found data on lake-specific volumetric outflow rate, it was too late to recalibrate the model. These two kinds of parameter are qualitatively different. While parameters that govern Hg transport may reasonably be assumed to be the same within a region, it is quite likely that volumetric outflow rate will differ for each lake. One might think of the calibrated volumetric outflow rate as an average value typical for the Maine region, with each lake varying around it. Although the methodology developed was correct, were there enough time, we would recalibrate the lakes without trying to optimize the volumetric outflow rate.

6.1.1. Volumetric outflow rate

The volumetric outflow rate in Hendricks (2018) varied seasonally and it had an average value of 278,918 m^3 day^{-1}. It should be noted that in this study seasonal variations were not taken into account. The calibrated value for the Maine lakes found in this study is 35.85% of the average value in Hendricks (2018). In reality, it is likely that each lake has a different outflow rate. However, given the location of these lakes in the same lake district with similar hydrology (EPA, 2009), they may have similar outflow rates. Dividing the volumes of each lake by this outflow rate yields a maximum retention time – the e-folding

time of the water in a lake - of 18.8 years for Grand, and a minimum retention time of 1.38 days for Sly Brook lake. This minimum value seems too low, suggesting that the optimal value over all the lakes for the outflow rate is too large, at least for some of the lakes. A larger outflow rate allows more pollutant sinking because it transports more Hg-contaminated water out of the lake. Thus, overestimated values of outflow rate would lead to decreased Hg concentrations compared to the reality.

6.1.2. Settling velocity

In Hendricks (2018), the settling velocity used for Torch Lake was 0.901 m day^{-1}. This value was calculated specifically for Torch Lake in Hendricks (2018). The calibrated value found in this study showed a 33.19% increase from the value in Hendricks (2018). The settling velocity controls particle transport from the hypolimnion to the surface sediments. An increase in settling velocity could allow more transport of Hg(II) to the sediments, where methylation will occur at a different rate than in the hypolimnion. Depending on the particular characteristics of a lake, this increased transport may lead to an increase or decrease in methylation, and thus in MeHg concentration. In Hendricks (2018), the water column methylation rate constant is 0.1 day^{-1}, while the methylation rate constant in the sediment is 0.0007 day^{-1}. Thus, an increase in particle transport velocity would decrease methylation and MeHg concentrations for the calibration used by Hendricks (2018).

6.1.3. Burial velocity

Hendricks (2018) uses a burial velocity of 6.1×10^{-6} m day^{-1}, calculated specifically for Torch Lake. The optimized value found by this study is 5.74% reduced from the value in Hendricks (2018). Burial velocity controls transport from the surface sediments to the

deep sediments. Because methylation will not occur appreciably in the deep sediments, a decreased burial velocity will increase MeHg concentrations, all else equal. The similarity of the value found by this study and the value in Hendricks (2018) suggests that those factors controlling burial velocity are similar for Torch Lake and the Maine lakes studied here.

6.1.4. Hg(II) biotic solids partitioning coefficient

This study found an optimal Hg(II) biotic solids partitioning coefficient of 0.4 L mg^{-1}, compared to a value in Hendricks (2018) of 0.9 L mg^{-1}, taken from Knightes (2008). This change constitutes a 55.5% increase in value. This partitioning coefficient is a ratio of Hg(II) concentration in the biotic solids phase to Hg(II) concentration in the dissolved phase. An increase in value represents increased sorption at equilibrium of Hg(II) on to biotic solids, reducing the ability of these Hg(II) (bound) ions to be methylated by sulfate- and iron-reducing bacteria, leading ultimately to a decrease in MeHg concentration. A lower partitioning coefficient speaks to a reduced capacity for sorption onto biotic solids, and it may suggest that in Maine's lakes the biotic solids are qualitatively different from those in Michigan, such that they form a poorer substrate for Hg sorption. Hg(II), as a positively charged species, would sorb especially well to a negative substrate. Perhaps the lower partitioning coefficient indicates that pH is lower in Maine as compared to Michigan. An environment relatively enriched in protons would lead to more positively charged biotic material that is worse for sorption. This interpretation is consonant with the increased alkalinity of the limestone-laden Midwest as compared to the granite-grounded Northeast.

6.2. Policy scenarios

A box-and-whiskers plot of modeled piscivore median MeHg concentrations in 1993 and under the three projected scenarios is shown in Figure 6.1. The CP (Current Policy) scenario is nearly indistinguishable from the MeHg concentrations in 1993. For the 1993 values, the median was 0.23 mg/L WW, while for the CP scenario, the median was 0.22 mg/L WW, and for both CP and 1993, the standard deviation of values was also equal to 0.22 mg/L WW. This finding indicates that if the world's nations merely maintain the Hg regulations which they had implemented or planned to implement in 2010, then the value of those regulations will have been vitiated in 2035 by the increased Hg pollution associated with larger populations and greater global affluence. The NP and MFR scenarios offer increasingly reduced MeHg concentrations due to stricter regulations.

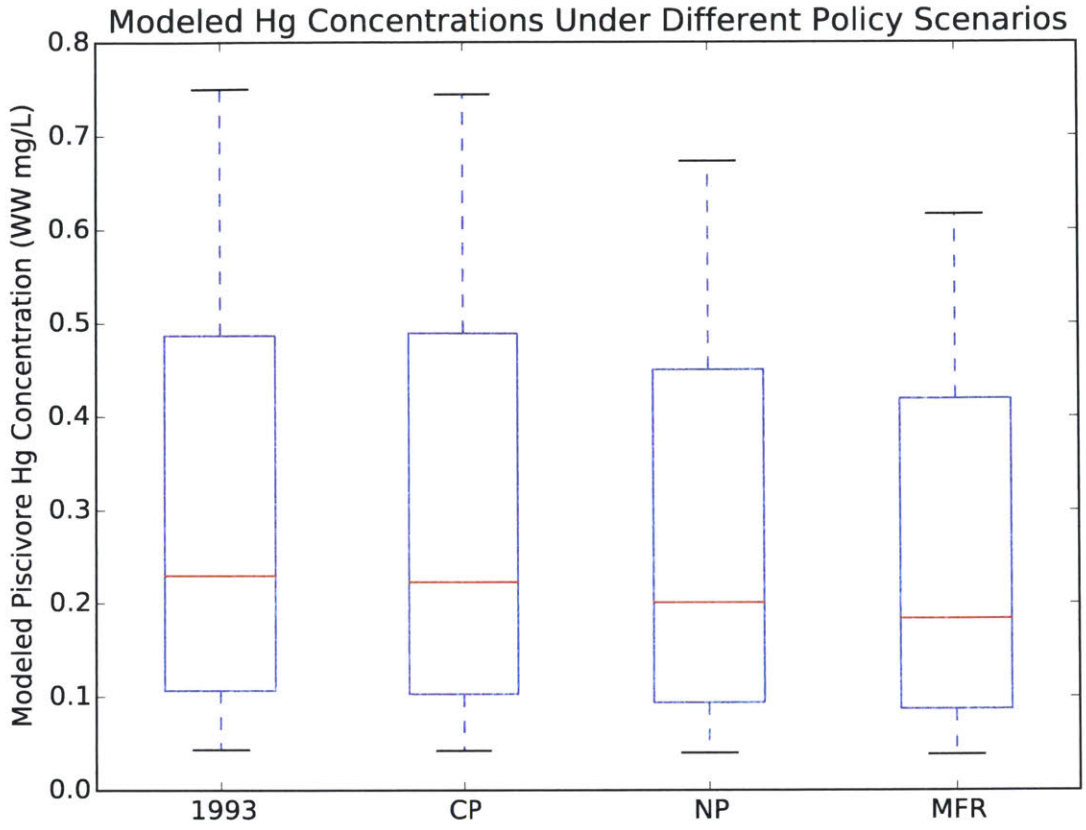

Figure 6.1: MeHg concentrations in fish in 1993 and three policy scenarios. There is little difference between 1993 values and current policy values. The MFR scenario leads to the greatest decrease in MeHg concentration.

In general, lakes with greater initial MeHg concentrations show more dramatic decreases in the three scenarios than those lakes with low MeHg concentrations to start with, as shown in Figure 6.2. This finding suggests that there may be diminishing returns from reducing MeHg concentrations: at lower concentrations of MeHg, stricter regulations are required, to produce the same marginal decrease in MeHg as at higher concentrations. However, greater decreases for lakes with higher MeHg concentrations are not observed strictly. Chase Lake was modeled as having the 3rd highest MeHg concentration in 1993, but its MeHg concentration actually increased under the CP scenario. This inter-lacustrine

variability suggests that differential sensitivity among the lakes to Hg deposition plays an important role in mediating the effect of changing Hg emissions on MeHg concentration. Lakes with higher ratios of lake and catchment surface area to lake volume may be particularly sensitive to Hg deposition.

As shown in Table 5.2, total Hg deposition is actually higher in the CP scenario (21.17 $\mu g/m^2$/year) as compared to the 1993 scenario (19.31 $\mu g/m^2$/year). One might expect, based on that difference for MeHg concentrations to be higher across the board in the CP scenario as compared to the 1993 scenario due to this fact. However, the data show that only two lakes (Chase and Keene) actually increase in the CP scenario, while all other lakes fall slightly in their median piscivore MeHg concentration. These slight reductions must be due to the fact that for the wet component of deposition, 1993 has higher values than CP. These lakes must be simulated as more sensitive to wet deposition than dry deposition in most cases. Chase is the smallest lake, with a small percentage of wetlands by area in its catchment. Wetlands are parametrized in the model with a reduced runoff coefficient, so Chase's smaller amount of wetlands leads to increased runoff in general, allowing the larger dry component of Hg deposition to dominate for this lake.

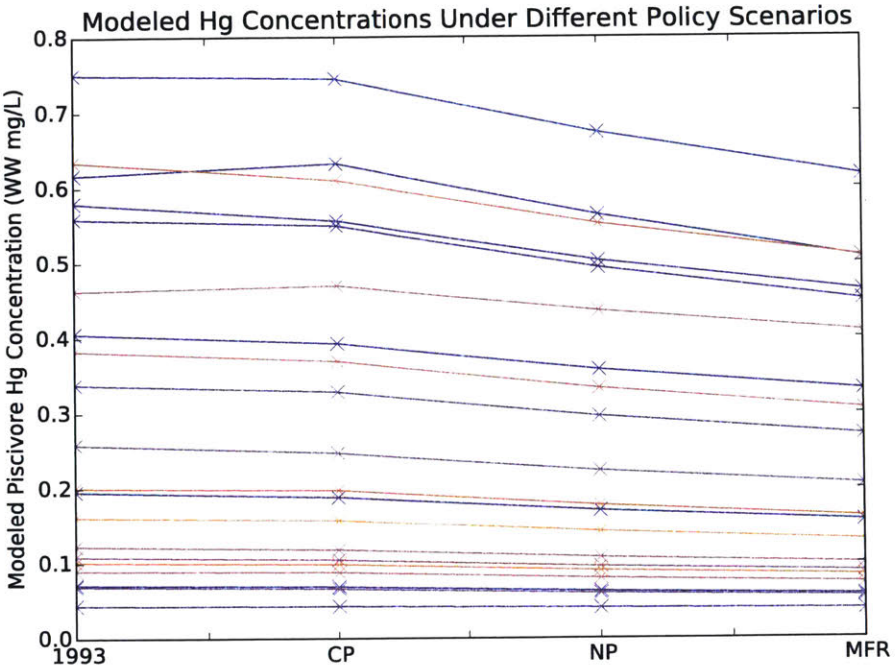

Figure 6.2: Line plots of MeHg change by lake. In general, lakes with greater initial concentrations of MeHg show more dramatic decreases.

6.3. Wabanaki subsistence

Gagnon et al. (2017) and Perlinger et al. (2018) detail how a local Michigan community helped define for themselves a desirable level of fish consumption as two 8 oz meals per day, which requires Hg concentrations of 0.015 ppm or less in order to be below the EPA reference dose of 0.1 $\mu g\ kg^{-1}\ day^{-1}$, the maximum daily level of safe exposure to MeHg. None of the lakes modeled meet this level of safe consumption for median piscivore concentrations, even under the strictest MFR scenario. The lake which comes closest is Monson, with a modeled median piscivore MeHg concentration of 0.0383 ppm, a value 155.33% greater than the safe value derived by Gagnon et al. (2017) and Perlinger et al. (2018). Even at the 5th percentile, Monson's piscivore Hg concentrations are 0.0186 ppm. However, Monson's 75th percentile of MeHg concentrations for mixed feeders is at 0.0146

ppm. These concentrations under the MFR scenario indicate that, even under the strictest global Hg regulations, a traditional-subsistence diet high in piscivores will lead to unhealthy MeHg exposure among the Wabanaki, while a diet that shifts toward mixed feeders will reduce MeHg exposure and may even be below EPA level of concern for particularly clean lakes under the strictest regulatory regime (see Figure 6.3) . However, one should be careful about recommending Wabanaki dietary shifts to mixed feeders (e.g. herring and white sucker) as a means of reducing MeHg exposures. Requiring the Wabanaki to change their diet because of changes made to their environment from remote sources is unfair. Thus, from the standpoint of environmental justice, the solution to the problem of elevated MeHg in fish is dramatic and speedy regulation, with the aim to create healthy fish conditions as soon as possible. In the interim, people who want to pursue the traditional-subsistence diet can use the results of this study to make an informed decision on the trade-off between health and cultural self-determination. This study makes no recommendation to the Wabanaki on whether or not to continue to eat fish with high MeHg concentrations at high frequencies. Rather, it presents the current and future MeHg concentrations in tribal fish and allows them to make their own decisions based on their own priorities.

It should also be noted that the Aroostook band of Micmacs, who live in Presque Isle, has created, in partnership with the US Fish and Wildlife Services, a recirculating aquaculture brook trout fish hatchery (USFWS, 2017). Although this contaminant-free source of brook trout is not a true substitute for a pristine environment, it offers an alternative source of healthy fish until MeHg concentrations in the environment are low enough for healthy consumption.

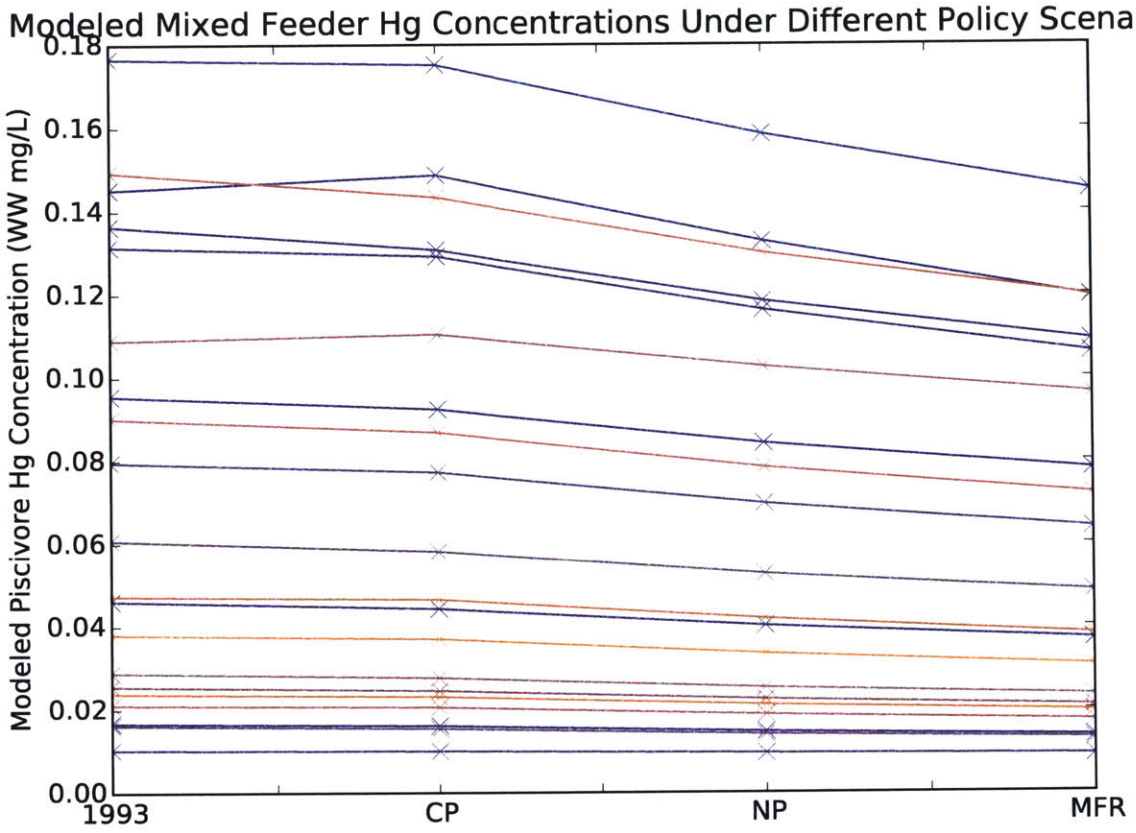

Figure 6.3: Median MeHg concentrations in mixed feeder fish for each lake under each scenario. Median mixed feeder MeHg concentrations will strictly be lower than piscivore median concentrations for all lakes in all scenarios. (Compare with Figure 5.2.)

6.4. Limitations

The execution of this study was hindered by the intrinsic complexity of Hg transport and fate in lake ecosystems. As shown in Figure 4.1, the system is modulated by many processes whose magnitude and direction may be lake-specific and time-varying. Even small uncertainties in the values that parametrize these processes in the model developed by Hendricks (2018) can act synergistically to produce substantial inaccuracies in the modeled result. This potential for uncertainty coupled to the lack of data on many processes makes it difficult to produce accurate results with the model.

This study was also limited by the fact that MeHg concentrations in Maine's lake fish were only recorded for the year 1993. Calibrating the model to these lakes for a single year may lead to inaccuracies in projected results, if the year chosen happens to be anomalous. Given the complexity of lacustrine fate and transport of Hg, anomalies could be produced by spikes in any number of parameters, such as unusually high precipitation (increasing wet deposition), high temperature, or increased solar activity leading to greater levels of photosynthetically active radiation. Were we to have had access to MeHg data for more years, we could have calibrated the model more robustly.

Similarly, this study was limited by small number of fish samples taken from each lake. For most lakes in this study, there was only one data point for piscivore whole fish concentration, produced by composite of 4 or 5 individual fish. These 4 or 5 fish taken from each lake may have had anomalous levels of MeHg concentration for any number of reasons. Had we more data points for each lake, we could have investigated variability of MeHg concentrations within the lakes and had a better sense of the actual pollutant profile of each lake.

Still, though the model contains many uncertainties, the conclusion that recovery will not follow quickly after implementation of Hg policies modeled in this study is robust.

6.5 Future research

We recommend, in order to better constrain the processes affecting Hg fate and transport, that more data be collected on these processes (e.g. particle transport velocities, equilibrium phase partitioning coefficients, oxidation/reduction and methylation/demethylation rate constants). The data should be collected in regions with different environmental conditions and during different times of year in order to more

accurately characterize the spatial and temporal variation of these processes. Specifically, the focus ought to be on more replications in each location

Additionally, the model should be evaluated for more lakes with different environmental conditions in order to test its versatility. If the lakes chosen have more data collected on them than those used in the present study, it may be easier to accurately calibrate the model, which could result in calibrations whose optimal values are more reliable than the ones calculated in the current study.

VII. REFERENCES

Achá, D., Hintelmann, H., & Yee, J. (2011). Importance of sulfate-reducing bacteria in mercury methylation and demethylation in periphyton from Bolivian Amazon region. *Chemosphere*, *82*(6), 911–916. http://doi.org/10.1016/j.chemosphere.2010.10.050

Agnan, Y., Le Dantec, T., Moore, C. W., Edwards, G. C., & Obrist, D. (2016). New constraints on terrestrial surface-atmosphere fluxes of gaseous elemental mercury using a global database. *Environmental Science and Technology*, *50*(2), 507–524. http://doi.org/10.1021/acs.est.5b04013

Allison, J. D., & Allison, T. L. (2005). Partition coefficients for metals in surface water, soil, and waste. *U.S. Environmental Protection Agency. Office of Research and Development*, (July), 93.

AMAP Assessment 2015: Human Health in the Arctic. Arctic Monitoring and Assessment Programme (AMAP), Oslo, Norway. 165 p.

Ambrose, R. B., Jr., Tsiros, I. X., & Wool, T. A. (2005). Modeling mercury fluxes and concentrations in a Georgia watershed receiving atmospheric deposition load from

direct and indirect sources. *Journal of the Air & Waste Management Association, 55*(5), 547-58.

Amos, H. M., Jacob, D. J., Holmes, C. D., Fisher, J. A., Wang, Q., Yantosca, R. M., & Sunderland, E. M. (2012). Gas-particle partitioning of atmospheric Hg(II) and its effect on global mercury deposition. *Atmospheric Chemistry and Physics*, *12*(1), 591–603. http://doi.org/10.5194/acp-12-591-2012

Amos, H. M., Jacob, D. J., Streets, D. G., & Sunderland, E. M. (2013). Legacy impacts of all-time anthropogenic emissions on the global mercury cycle. *Global Biogeochemical Cycles, 27*(2), 410–421. http://doi.org/10.1002/gbc.20040

Angot, H., Hoffman, N., Selin, N. E., & Giang, A. (In prep). The consequences of delayed global action on policy impacts and local mercury contamination. To be submitted to *Environmental Science and Technology*.

Asch Sidell, N. (1999). Prehistoric plant use in Maine: Paleoindian to Contact Period. Chapter 12 in *Current Northeast Paleoethnobotany I* (Hart, J.P. ed). New York State Museum, The University of the State of New York.

Barkay, T., Gillman, M., Turner, R. R., & Gillman, M. (1997). Effects of dissolved organic carbon and salinity on bioavailability of mercury, *Applied and Environmental Microbiology, 63*(11), 4267–4271.

Black, F.J., Poulin, B.A., & Flegal, A.R. (2012). Factors controlling the abiotic photo-degradation of methylmercury in surface waters. *Geochimica et Cosmochimica Acta, 84,* 492-507.

Boening, D. W. (2000). Ecological effects, transport, and fate of mercury: A general review. *Chemosphere*, *40*(12), 1335–1351. http://doi.org/10.1016/S0045-6535(99)00283-0

Branfireun, B. A, Roulet, N. T., Kelly, A I., & Rudd, J. W. M. (1999). *In situ* stimulation of mercury methylation in a boreal peatland: Toward a link between acid rain and methylmercury contamination in remote environments, *Global Biogeochemical Cycles 13*(3), 743–750.

Celo, V., Lean, D. R. S., & Scott, S. L. (2006). Abiotic methylation of mercury in the aquatic environment. *Science of the Total Environment, 368*(1), 126–137. http://doi.org/10.1016/j.scitotenv.2005.09.043

Chételat, J., Amyot, M., & Garcia, E. (2011). Habitat-specific bioaccumulation of methylmercury in invertebrates of small mid-latitude lakes in North America. *Environmental Pollution, 159*(1), 10–17. http://doi.org/10.1016/j.envpol.2010.09.034

Cooke, C. A, Balcom, P. H., Biester, H., & Wolfe, A. P. (2009). Over three millennia of mercury pollution in the Peruvian Andes. *Proceedings of the National Academy of Sciences of the United States of America, 106*(22), 8830–4. http://doi.org/10.1073/pnas.0900517106

Correia, R. R., Miranda, M. R., & Guimaraes, J. R. (2011). Mercury methylation and the microbial consortium in periphyton of tropical macrophytes: Effect of different inhibitors. *Environmental Research*.

Dieffenbacher-Krall, A. C., & Nurse, A. M. (2005). Late-glacial and Holocene record of lake levels of Mathews Pond and Whitehead Lake, northern Maine, USA. *Journal of Paleolimnology, 34*(3), 283–309. http://doi.org/10.1007/s10933-005-4958-8

Eagles-Smith, C. A., Silbergeld, E. K., Basu, N., Bustamante, P., Diaz-Barriga, F., Hopkins, W. A., & Nyland, J. F. (2018). Modulators of mercury risk to wildlife and humans in the context of rapid global change. *Ambio, 47*(2), 170–197. http://doi.org/10.1007/s13280-017-1011-x

Eckley, C. S., Watras, C. J., Hintelmann, H., Morrison, K., Kent, A. D., & Regnell, O. (2005). Mercury methylation in the hypolimnetic waters of lakes with and without connection to wetlands in northern Wisconsin. *Canadian Journal of Fisheries and Aquatic Sciences, 62*(2), 400–411. http://doi.org/10.1139/f04-205

Eckley, C. S., & Hintelmann, H. (2006). Determination of mercury methylation potentials in the water column of lakes across Canada. *Science of the Total Environment, 368*(1), 111–125. http://doi.org/10.1016/j.scitotenv.2005.09.042

Engstrom, D. R. (2007). Fish respond when the mercury rises. *Proceedings of the National Academy of Sciences, 104*(42), 16394–16395. http://doi.org/10.1073/pnas.0708273104

EPA. (1997). *Mercury Study Report to Congress, Volume III: Fate and Transport of Mercury in the Environment.* Office of Air Quality Planning and Standards, and Office of Research and Development.

EPA. (2009). Wabanaki Traditional Cultural Lifeways Exposure Scenario - DITCA. *EPA.* Presented by Darren Ranco.

Ferrara, R., Mazzolai, B., Lanzillotta, E., Nucaro, E., & Pirrone, B. (2000). Volcanoes as emission sources of atmospheric mercury in the Mediterranean basin. *Science of the Total Environment, 259,* 115-121.

Fitzgerald, W. F., Lamborg, C. H., & Hammerschmidt, C. R. (2007). Marine Biogeochemical cycling of mercury. *Chemical Reviews, 107*(2), 641–662. http://doi.org/10.1021/cr050353m

Fitzgerald, W. F., & Lamborg, C. H. (2013). *Geochemistry of Mercury in the Environment. Treatise on Geochemistry: Second Edition* (11th ed., Vol. 11). Elsevier Ltd. http://doi.org/10.1016/B978-0-08-095975-7.00904-9

Fu, X., Marusczak, N., Heimbürger, L. E., Sauvage, B., Gheusi, F., Prestbo, E. M., & Sonke, J. E. (2016). Atmospheric mercury speciation dynamics at the high-altitude Pic du Midi Observatory, southern France. *Atmospheric Chemistry and Physics, 16*(9), 5623–5639. http://doi.org/10.5194/acp-16-5623-2016

Gagnon, V., Gorman, H., & Norman, E. (2017). Power and politics in research design and practice: Opening up space for social equity in interdisciplinary, multi-jurisdictional and community-based research. *Gateways: International Journal of Community Research and Engagement*, vol. 10, pp. 164–184. doi: 10.5130/ijcre.v10i1.5307

Gionfriddo, C. M., Tate, M. T., Wick, R. R., Schultz, M. B., Zemla, A., Thelen, M. P., & Moreau, J. W. (2016). Microbial mercury methylation in Antarctic sea ice. *Nature Microbiology, 1*(August), 1–12. http://doi.org/10.1038/nmicrobiol.2016.127

Grandjean P., Satoh H., Murata K., & Eto K. (2010). Adverse effects of methylmercury: Environmental health research implications. *Environmental Health Perspectives, 118.* 1137-45.

Gustin, M., Lindberg, S., Austin, K., Coolbaugh, M., Vette, A., & Zhang, H. (2000). Assessing the contribution of natural sources to regional atmospheric mercury budgets. *The Science of the Total Environment, 259*(1-3), 61–71. http://doi.org/http://dx.doi.org/10.1016/S0048-9697(00)00556-8

Hall, B. D., Manolopoulos, H., Hurley, J. P., Schauer, J. J., St. Louis, V. L., Kenski, D., & Keeler, G. J. (2005). Methyl and total mercury in precipitation in the Great Lakes region.

Atmospheric Environment, *39*(39 SPEC. ISS.), 7557–7569. http://doi.org/10.1016/j.atmosenv.2005.04.042

Hamelin, S., Amyot, M., Barkay, T., Wang, Y., & Planas, D. (2011). Methanogens: Principal methylators of mercury in lake periphyton. *Environmental Science and Technology, 45*(18), 7693-7700.

Hamelin, S., Planas, D., & Amyot, M. (2015). Mercury methylation and demethylation by periphyton biofilms and their host in a fluvial wetland of the St. Lawrence River (QC, Canada). *Science of the Total Environment*, *512-513*, 464–471. http://doi.org/10.1016/j.scitotenv.2015.01.040

Hammerschmidt, C. R., & Fitzgerald, W. F. (2004). Geochemical controls on the production and distribution of methylmercury in near-shore marine sediments. *Environmental Science and Technology*, *38*(5), 1487–1495. http://doi.org/10.1021/es034528q

Hammerschmidt, C. R., & Fitzgerald, W. F. (2006). Bioaccumulation and trophic transfer of methylmercury in Long Island Sound. *Archives of Environmental Contamination and Toxicology*, *51*(3), 416–424. http://doi.org/10.1007/s00244-005-0265-7

Hendricks, A. (2018) A model to predict concentrations and uncertainty for mercury species in lakes. (Unpublished Masters Thesis). Michigan Technological University, Houghton, Michigan, USA.

Hintelmann, H., Keppel-Jones, K., & Evans, R. D. (2000). Constants of mercury methylation and demethylation rates in sediments and comparison of tracer and ambient mercury availability. *Environmental Toxicology and Chemistry*, *19*(9), 2204–2211. http://doi.org/10.1002/etc.5620190909

Hintelmann, H., Harris, R., Heyes, A., Hurley, J. P., Kelly, C. a., Krabbenhoft, D. P., & St. Louis, V. L. (2002). Reactivity and mobility of new and old mercury deposition in a boreal forest ecosystem during the first year of the METAALICUS study. *Environmental Science and Technology*, *36*(23), 5034–5040. http://doi.org/10.1021/es025572t

Holmes, C. D., Jacob, D. J., Corbitt, E. S., Mao, J., Yang, X., Talbot, R., & Slemr, F. (2010). Global atmospheric model for mercury including oxidation by bromine atoms. *Atmospheric Chemistry and Physics*, *10*(24), 12037–12057. http://doi.org/10.5194/acp-10-12037-2010

Horowitz, H. M., Jacob, D. J., Zhang, Y., DIbble, T. S., Slemr, F., Amos, H. M., & Sunderland, E. M. (2017). A new mechanism for atmospheric mercury redox chemistry: Implications for the global mercury budget. *Atmospheric Chemistry and Physics*, *17*(10), 6353–6371. http://doi.org/10.5194/acp-17-6353-2017

Jensen, S., & Jernelöv, A. (1969). Biological methylation of mercury in aquatic organisms. *Nature*, *223*(5207), 753–754. http://doi.org/10.1038/223753a0

Johnson, N. W., Mitchell, C. P. J., Engstrom, D. R., Bailey, L. T., Wasik, J. K. C., & Berndt, M. E. (2016). Methylmercury production in a chronically sulfate impacted sub-boreal wetland. *Royal Society of Chemistry, 18*, 725-734.

Jones, D. S. (2003). Virgin soils revisited. *The William and Mary Quarterly*, *60*(4), 703-742.

Jonsson, S., Skyllberg, U., Nilsson, M. B., Lundberg, E., Andersson, A., & Björn, E. (2014). Differentiated availability of geochemical mercury pools controls methylmercury levels in estuarine sediment and biota. *Nature Communications*, *5*, 4624. http://doi.org/10.1038/ncomms5624

Klapstein, S. J., & O'Driscoll, N. J. (2017). Methylmercury biogeochemistry in freshwater ecosystems: A review focusing on DOM and photodemethylation. *Bulletin of Environmental Contamination and Toxicology*. http://doi.org/10.1007/s00128-017-2236-x

Klapstein, S. J., Ziegler, S. E., Risk, D. A., & O'Driscoll, N. J. (2017). Quantifying the effects of photoreactive dissolved organic matter on methylmercury photodemethylation rates in freshwaters. *Environmental Toxicology and Chemistry*, *36*(6), 1493–1502. http://doi.org/10.1002/etc.3690

Knightes, C. D. (2008). Development and test application of a screening-level mercury fate model and tool for evaluating wildlife for surface waters with mercury-contaminated sediments (SERAFM). *Environmental Modelling and Software, 23*(4). 495-510.

Knightes, C. D., Sunderland, E. M., Barber, M. C., Johnston, J. M., & Ambrose, R. B. (2009). Hazard/Risk Assessment: Application of ecosystem-scale fate and bioaccumulation models to predict fish mercury response times to changes in atmospheric deposition. *Environmental Toxicology and Chemistry*, *28*(4), 881–893. http://doi.org/10.1897/08-242R.1

Korthals, E. T., & Winfrey, M. R. (1987). Seasonal and spatial variations in mercury methylation and demethylation in an oligotrophic lake. *Applied and Environmental Microbiology*, *53*(10), 2397–404.

Kuss, J., Holzmann, J., & Ludwig, R. (2009). An elemental mercury diffusion coefficient for natural waters determined by molecular dynamics simulation. *Environmental Science & Technology*, *43*(9), 3183–3186. http://doi.org/10.1021/es8034889

Lin, C. J., & Pehkonen, S. O. (1999). The chemistry of atmospheric mercury: A review. *Atmospheric Environment*, *33*(13), 2067–2079. http://doi.org/10.1016/S1352-2310(98)00387-2

Lindberg, S. E., Meyers, T. P., & Taylor Jr, G. . (1992). Atmosphere-surface exchange of mercury in a forest: results of modeling and gradient approaches. *Atmos. Environ.*, *32*(12), 3897–3917.

Lindberg, S. E., & Stratton, W. J. (1998). Atmospheric mercury speciation: Concentration and behavior of reactive gaseous mercury in ambient air. *Environmental Science and Technology*, *32*(1), 49–57. http://doi.org/10.1021/es970546u

Lindberg, S., Bullock, R., Ebinghaus, R., Engstrom, D., Feng, X., Fitzgerald, W., & Seigneur, C. (2007). A synthesis of progress and uncertainties in attributing the sources of mercury in deposition. *Ambio*, *36*(1), 19–32. http://doi.org/10.1579/0044-7447(2007)36[19:ASOPAU]2.0.CO;2

Lindqvist, O., & Rodhe, H. (1985). Atmospheric mercury—a review. *Tellus B*, *37 B*(3), 136–159. http://doi.org/10.1111/j.1600-0889.1985.tb00062.x

Lyon, B. F., Ambrose, R., Rice, G., & Maxwell, C. J. (1997). Calculation of soil-water and benthic sediment partition coefficients for mercury. *Chemosphere 35*(4). 791-808.

Maine Department of Environmental Protection. (1995). Fish tissue contamination in Maine lakes data report. *Regional Environmental Monitoring and Assessment Program*. By DiFranco, J., Bacon, L., Mower, B., & Courtemanch, D.

Mason, R. P., & Sheu, G.-R. (2002). Role of the ocean in the global mercury cycle. *Global Biogeochemical Cycles*, *16*(4), 40–1–40–14. http://doi.org/10.1029/2001GB001440

Muntean, M., Janssens-Maenhout, G., Song, S., Selin, N. E., Olivier, J. G. J., Guizzardi, D., & Dentener, F. (2014). Trend analysis from 1970 to 2008 and model evaluation of EDGARv4 global gridded anthropogenic mercury emissions. *Science of the Total Environment, 494-495*, 337–350. http://doi.org/10.1016/j.scitotenv.2014.06.014

National Emissions Inventory. 2011. https://www.epa.gov/air-emissions-inventories/2011-national-emissions-inventory-nei-data

National Hydrography Dataset. https://nhd.usgs.gov/NHD_High_Resolution.html

National Wetlands Inventory. Wetlands Mapper. https://www.fws.gov/wetlands/Data/Mapper.html

Nagase, H., Ose, Y., Sato, T., & Ishikawa, T. (1984). Mercury methylation by compounds in humic material. *The Science of the Total Environment, 32*, 147–156.

National Atmospheric Deposition Program. http://nadp.slh.wisc.edu/NADP/.

Nriagu, J. O. (1993). Legacy of mercury pollution. *Nature*. http://doi.org/10.1038/363589a0

O'Driscoll, N. J., Vost, E., Mann, E., Klapstein, S., Tordon, R., & Lukeman, M. (2017). Mercury photoreduction and photooxidation in lakes: Effects of filtration and dissolved organic carbon concentration. *Journal of Environmental Sciences*, (Ii), 1–9. http://doi.org/10.1016/j.jes.2017.12.010

O'Neill, C. Mercury, Risk, and Justice. (2004). *Environmental Law Reporter, 34*(12). https://ssrn.com/abstract=1004769

Pacyna, E. G., & Pacyna, J. M. (2002). Global emissions of mercury from anthropogenic sources in 1995. *Water, Air, and Soil Pollution, 137*, 149–165. http://doi.org/http://dx.doi.org/10.1016/S1352-2310(01)00102-9

Pacyna, J. M., Travnikov, O., Simone, F. De, Hedgecock, I. M., Sundseth, K., Pacyna, E. G., & Kindbom, K. (2016). Current and future levels of mercury atmospheric pollution on a global scale. *Atmospheric Chemistry and Physics*, *16*(19), 12495–12511. http://doi.org/10.5194/acp-16-12495-2016

Parks, J. M., Johs, A., Podar, M., Bridou, R., Hurt, R. a., Smith, S. D., & Liang, L. (2013). The genetic basis for bacterial mercury methylation. *Science*, *339*(6125), 1332–1335. http://doi.org/10.1126/science.1230667

Paranjape, A. R., & Hall, B. D. (2017). Recent advances in the study of mercury methylation in aquatic systems. *Facets*, *2*(1), 85–119. http://doi.org/10.1139/facets-2016-0027

Perlinger, A., Urban, N.R., Giang, A., Selin, N.E., Hendricks, A.N., Zhang, H., Kumar, A., Wu, S., Gagnon, V.S., Gorman, H.S., & Norman, E.S. (2018). An approach to model the time to fish consumption safe from methylmercury exposure in a tribal community. *Environmental Science: Processes and Impacts.*

Poissant, L., Pilote, M., Beauvais, C., Constant, P., & Zhang, H. H. (2005). A year of continuous measurements of three atmospheric mercury species (GEM, RGM and Hg(P)) in southern Québec, Canada. *Atmospheric Environment, 39*(7), 1275-1287. doi:http://dx.doi.org/10.1016/j.atmosenv.2004.11.007

Poissant, L., Pilote, M., Yumvihoze, E., & Lean, D. (2008). Mercury concentrations and foliage/atmosphere fluxes in a maple forest ecosystem in Québec, Canada. *Journal of Geophysical Research Atmospheres*, *113*(10), 1–12. http://doi.org/10.1029/2007JD009510

Poste, A. E., Braaten, H. F. V., de Wit, H. A., Sørensen, K., & Larssen, T. (2015). Effects of photodemethylation on the methylmercury budget of boreal Norwegian lakes.

Environmental Toxicology and Chemistry, *34*(6), 1213–1223. http://doi.org/10.1002/etc.2923

Prestbo, E. M., & Gay, D. A. (2009). Wet deposition of mercury in the U.S. and Canada, 1996-2005: Results and analysis of the NADP mercury deposition network (MDN). *Atmospheric Environment*, *43*(27), 4223–4233. http://doi.org/10.1016/j.atmosenv.2009.05.028

Prins, H. E. L., & McBride, B. (2007). *Asticou's Island Domain: Wabanaki Peoples at Mount Desert Island: 1500-2000: Ethnographic Overview and Assessment, Volume I.* Acadia National Park.

Ranco, D. J., O'Neill, C. a., Donatuto, J., & Harper, B. L. (2011). Environmental justice, American Indians and the cultural dilemma: Developing environmental management for tribal health and well-being. *Environmental Justice*, *4*(4), 221–230. http://doi.org/10.1089/env.2010.0036

Ravichandran, M. (2004). Interactions between mercury and dissolved organic matter - A review. *Chemosphere*, *55*(3), 319–331. http://doi.org/10.1016/j.chemosphere.2003.11.011

Rolfhus, K. R., Hall, B. D., Monson, B. A., Paterson, M. J., & Jeremiason, J. D. (2011). Assessment of mercury bioaccumulation within the pelagic food web of lakes in the western Great Lakes region. *Ecotoxicology*, *20*(7), 1520–1529. http://doi.org/10.1007/s10646-011-0733-y

Sando, S. K., & Cates, S. W. (1994). Determination of sediment thickness and volume in Lake Byron, South Dakota, using continuous seismic-reflection methods. USGS.

Santschi, P. H., Yeager, K. M., Schwehr, K. a., & Schindler, K. J. (2017). Estimates of recovery of the Penobscot River and estuarine system from mercury contamination in the 1960s. *Science of the Total Environment, 596-597*, 351–359. http://doi.org/10.1016/j.scitotenv.2017.04.094

Schartup, A. T., Qureshi, A., Dassuncao, C., Thackray, C. P., Harding, G., & Sunderland, E. M. (2018). A model for methylmercury uptake and trophic transfer by marine plankton. *Environmental Science and Technology, 52*(2), 654–662. http://doi.org/10.1021/acs.est.7b03821

Selin, N. E., Jacob, D. J., Park, R. J., Yantosca, R. M., Strode, S., Jaeglé, L., & Jaffe, D. (2007). Chemical cycling and deposition of atmospheric mercury: Global constraints from observations. *Journal of Geophysical Research Atmospheres, 112*(2), 1–14. http://doi.org/10.1029/2006JD007450

Selin, N. E., & Jacob, D. J. (2008). Seasonal and spatial patterns of mercury wet deposition in the United States: Constraints on the contribution from North American anthropogenic sources. *Atmospheric Environment, 42*(21), 5193–5204. http://doi.org/10.1016/j.atmosenv.2008.02.069

Selin, N. E. (2009). Global biogeochemical cycling of mercury: A review. *Annual Review of Environment and Resources, 34*(1), 43–63. http://doi.org/10.1146/annurev.environ.051308.084314

Selin, N. E., Sunderland, E. M., Knightes, C. D., & Mason, R. P. (2010). Sources of mercury exposure for U.S. seafood consumers: Implications for policy. *Environmental Health Perspectives, 118*(1), 137–143. http://doi.org/10.1289/ehp.0900811

Shah, V., Jaeglé, L., Gratz, L. E., Ambrose, J. L., Jaffe, D. A., Selin, N. E., & Mauldin, R. L. (2016). Origin of oxidized mercury in the summertime free troposphere over the southeastern US. *Atmospheric Chemistry and Physics*, *16*(3), 1511–1530. http://doi.org/10.5194/acp-16-1511-2016

Shah, V., & Jaeglé, L. (2017). Subtropical subsidence and surface deposition of oxidized mercury produced in the free troposphere. *Atmospheric Chemistry and Physics*, *17*(14), 8999–9017. http://doi.org/10.5194/acp-17-8999-2017

Sommar, J., Gårdfeldt, K., Strömberg, D., & Feng, X. (2001). A kinetic study of the gas-phase reaction between the hydroxyl radical and atomic mercury. *Atmospheric Environment*, *35*(17), 3049–3054. http://doi.org/10.1016/S1352-2310(01)00108-X

Sprovieri, F., Pirrone, N., Bencardino, M., D'Amore, F., Carbone, F., Cinnirella, S., Mannarino, V., Landis, M., Ebinghaus, R., Weigelt, A., Brunke, E.-G., Labuschagne, C., Martin, L., Munthe, J., Wängberg, I., Artaxo, P., Morais, F., Barbosa, H. D. M. J., Brito, J., Cairns, W., Barbante, C., Diéguez, M. D. C., Garcia, P. E., Dommergue, A., Angot, H., Magand, O., Skov, H., Horvat, M., Kotnik, J., Read, K. A., Neves, L. M., Gawlik, B. M., Sena, F., Mashyanov, N., Obolkin, V., Wip, D., Feng, X. B., Zhang, H., Fu, X., Ramachandran, R., Cossa, D., Knoery, J., Marusczak, N., Nerentorp, M., and Norstrom, C. (2016). Atmospheric mercury concentrations observed at ground-based monitoring sites globally distributed in the framework of the GMOS network, *Atmospheric Chemistry and Physics, 16*, 11915-11935, https://doi.org/10.5194/acp-16-11915-2016.

Streets, D. G., Devane, M. K., Lu, Z., Bond, T. C., Sunderland, E. M., & Jacob, D. J. (2011). All-time releases of mercury to the atmosphere from human activities. *Environmental Science and Technology*, *45*(24), 10485–10491. http://doi.org/10.1021/es202765m

Streets, D. G., Horowitz, H. M., Jacob, D. J., Lu, Z., Levin, L., Ter Schure, A. F. H., & Sunderland, E. M. (2017). Total mercury released to the environment by human activities. *Environmental Science and Technology*, *51*(11), 5969–5977. http://doi.org/10.1021/acs.est.7b00451

Sunderland, E. M., Cohen, M. D., Selin, N. E., & Chmura, G. L. (2008). Reconciling models and measurements to assess trends in atmospheric mercury deposition. *Environmental Pollution*, *156*(2), 526–535. http://doi.org/10.1016/j.envpol.2008.01.021

Sunderland, E. M., Amirbahman, A., Burgess, N. M., Dalziel, J., Harding, G., Jones, S. H., & Chen, C. Y. (2012). Mercury sources and fate in the Gulf of Maine. *Environmental Research*, *119*(May), 27–41. http://doi.org/10.1016/j.envres.2012.03.011

Sunderland, E. M., Li, M., & Bullard, K. (2018). Decadal changes in the edible supply of seafood and methylmercury exposure in the United States. *Environmental Health Perspectives*, *126*(1), 1–6. http://doi.org/10.1289/EHP2644

Tjerngren, I., Karlsson, T., Björn, E., & Skyllberg, U. (2012). Potential Hg methylation and MeHg demethylation rates related to the nutrient status of different boreal wetlands. *Biogeochemistry*, *108*(1-3), 335–350. http://doi.org/10.1007/s10533-011-9603-1

Travnikov, O., Angot, H., Artaxo, P., Bencardino, M., Bieser, J., D'Amore, F., Dastoor, A., De Simone, F., Diéguez, M. D. C., Dommergue, A., Ebinghaus, R., Feng, X. B., Gencarelli, C. N., Hedgecock, I. M., Magand, O., Martin, L., Matthias, V., Mashyanov, N., Pirrone, N., Ramachandran, R., Read, K. A., Ryjkov, A., Selin, N. E., Sena, F., Song, S., Sprovieri, F., Wip, D., Wängberg, I., and Yang, X.: Multi-model study of mercury dispersion in the atmosphere: atmospheric processes and model evaluation, *Atmospheric Chemistry and Physics*, *17*, 5271-5295, https://doi.org/10.5194/acp-17-5271-2017, 2017.

Ullrich, S.M., Tanton, T.W., & Abdrashitova, S.A. (2001). Mercury in the aquatic environment: A review of factors affecting methylation. *Critical Reviews in Environmental Science and Technology, 31*, 241-293.

United Nations Environmental Programme. (2002). *Global Mercury Assessment.*

United Nations Environmental Programme. (2013a). *Global Mercury Assessment.*

United Nations Environmental Programme. (2013b). Minamata Convention on Mercury - Text and Annexes. *UNEP, 2013*, 69. http://doi.org/10.1016/j.apgeochem.2007.12.024

USFWS. (2017). First Micmac fish harvest. https://usfwsnortheast.wordpress.com/2017/06/28/first-micmac-fish-harvest/

Wang, S., Feng, X., Qiu, G., Wei, Z., & Xiao, T. (2005). Mercury emission to atmosphere from Lanmuchang Hg-Tl mining area, Southwestern Guizhou, China. *Atmospheric Environment, 39*(39 SPEC. ISS.), 7459–7473. http://doi.org/10.1016/j.atmosenv.2005.06.062

Warner, K. A., Roden, E. E., & Bonzongo, J. C. (2003). Microbial mercury transformation in anoxic freshwater sediments under iron-reducing and other electron-accepting conditions. *Environmental Science and Technology, 37*(10), 2159–2165. http://doi.org/10.1021/es0262939

Watershed Boundary Dataset. https://nhd.usgs.gov/wbd.html

Watras, C. J., Morrison, K. A., Host, J. S., & Bloom, N. S. (1995). Concentration of mercury species in relationship to other site-specific factors in the surface waters of northern Wisconsin lakes. *Limnology and Oceanography, 40*(3), 556–565. http://doi.org/10.4319/lo.1995.40.3.0556

Watras, C. J., Back, R. C., Halvorsen, S., Hudson, R. J. M., Morrison, K. A., & Wente, S. P. (1998). Bioaccumulation of mercury in pelagic freshwater food webs. *Science of the Total Environment, 219*(2-3), 183–208. http://doi.org/10.1016/S0048-9697(98)00228-9

WGME. (2017). Maine's pulp and paper industry by the numbers.

Wiener, J.G., Krabbenhoft, D.P., Heinz, G.H., & Scheuhammer, A.M., (2003). Ecotoxicology of mercury. In: Hoffman, D.J, Rattner, B.A., Burton, G.A. Jr., & Cairns J. Jr., (eds.). *Handbook of Ecotoxicology*. Lewish Publishers, Boca Raton, pp. 409-463.

Wolfe, M. F., Schwarzbach, S., & Sulaiman, R. A. (1998). Effects of mercury on wildlife: A comprehensive review. *Environmental Toxicology and Chemistry, 17*(2), 146–160. http://doi.org/10.1002/etc.5620170203

Wright, P. L., Zhang, L., & Marsik, F. J. (2016). Overview of mercury dry deposition, litterfall, and throughfall studies. *Atmospheric Chemistry and Physics, 16*(21), 13399–13416. http://doi.org/10.5194/acp-16-13399-2016

Xiao, Z. F., Munthe, J., & Lindqvist, O. (1991). Sampling and determination of gaseous and particulate mercury in the atmosphere using gold-coated denuders. *Water, Air, & Soil Pollution, 56*(1), 141–151. http://doi.org/10.1007/BF00342268

Yeager, K. M., Schwehr, K. A., Louchouarn, P., Feagin, R. A., Schindler, K. J., & Santschi, P. H. (2018). Mercury inputs and redistribution in the Penobscot River and estuary, Maine. *Science of the Total Environment, 622-623*, 172–183. http://doi.org/10.1016/j.scitotenv.2017.11.334

Zhang, L., Wright, L. P., & Blanchard, P. (2009). A review of current knowledge concerning dry deposition of atmospheric mercury. *Atmospheric Environment, 43*(37), 5853–5864. http://doi.org/10.1016/j.atmosenv.2009.08.019

Zhang, L., Wu, Z., Cheng, I., Wright, L. P., Olson, M. L., Gay, D. a., & Weiss-Penzias, P. (2016). The estimated six-year mercury dry deposition across North America. *Environmental Science & Technology*, *50*(23), 12864–12873. http://doi.org/10.1021/acs.est.6b04276

Zhu, S., Zhang, Z., & Liu, X. (2017). Enhanced two dimensional hydrodynamic and water quality model (CE-QUAL-W2) for simulating mercury transport and cycling in water bodies. *Water*, *9*(9), 643. http://doi.org/10.3390/w9090643

VIII. APPENDIX

Table 8.1. Lake Names. Highlighted lakes were part of the training set chosen for the calibration.

Lake	Number
Brackett	1
Bradbury	2
Chandler	3
Chase	4
Cross	5
Eagle	6
Grand	7
Keene	8
Lambert	9
Machias	10
Meddybemps	11
Molunkus	12
Monson	13
Orange	14
Pennington	15
Portland	16
Pleasant1	17
Sly Brook	18
Togue	19
Umcolcus	20

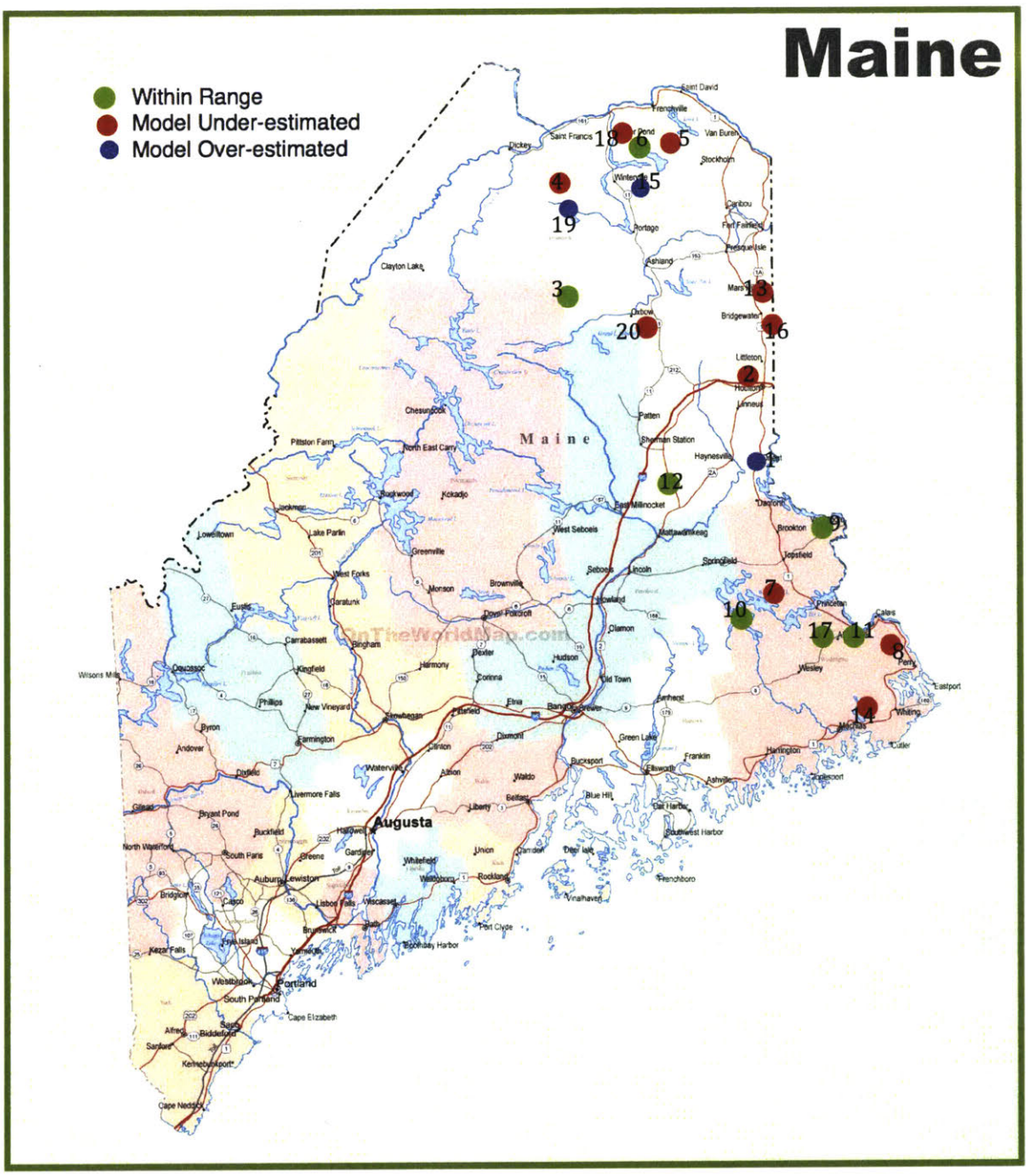

Figure 8.1: Lake Locations. The lakes all came from the eastern remove of Aroostook and Washington counties.

Table 8.2. Lake Attributes.

Lake	Surface Area (m^2)	Catchment Area (m^2)	Total Volume (m^3)	Total sediment Hg concentration (ppmm)	Average DOC concentration (ppmm)	Percent Wetland by Area
Brackett	2.29×10^6	1.9×10^7	9,513,420	0.002	2.9	5.31
Bradbury	160000	4.3×10^7	890,349	0.21	3.2	9.71
Chandler	1.68×10^6	1.2×10^7	5,742,808	0.12	2.1	10.89
Chase	4000	1.1×10^7	202,901	0.2	1.1	3.74
Cross	1.027×10^7	4.25×10^8	6.447034×10^7	0.12	1.15	30.31
Eagle	2.259×10^7	1.974×10^9	3.08×10^8	0.09	1.95	11.22
Grand	5.834×10^7	5.85×10^8	6.86×10^8	0.2	4.8	5.75
Keene	360000	4×10^6	650,251	0.21	4.1	10
Lambert	2.18×10^6	1.7×10^7	1.432766×10^7	0.31	3.45	16.53
Machias	6.2×10^6	1.72×10^8	2.05512×10^7	0.12	7.5	17.85
Meddybemps	2.718×10^7	1.16×10^8	1.18×10^8	0.18	3.65	19.28
Molunkus	4.36×10^6	9.1×10^7	1.850236×10^7	0.22	6.75	13.72
Monson	370000	3.8×10^7	729,505	0.13	6.75	16.02
Orange	930000	5×10^7	2,627,014	0.22	8.85	19.16
Pennington	210000	4×10^6	1.560627×10^7	0.09	3.6	18.38
Portland	166000	1.8×10^6	8,124,426	0.2	1.4	25.77
Pleasant1	1.4×10^6	8×10^6	7,353,291	0.11	1.65	19.28
Sly Brook	70000	7×10^6	137,983	0.17	1.1	7.66
Togue	1.3×10^6	9×10^6	1.560627×10^7	0.19	1	4.07
Umcolcus	2.9×10^6	3.8×10^7	8,124,429	0.14	3.05	20.86